This is a preprint of: "Flow map parameterization methods for invariant tori in quasi-periodic Hamiltonian systems", Álvaro Fernández-Mora, Àlex Haro, Josep Maria Mondelo, *SIAM J. Appl. Dyn. Syst.*, vol. 23(1), 127–166, 2024.
DOI: [10.1137/23M1561257]

FLOW MAP PARAMETERIZATION METHODS FOR INVARIANT TORI IN QUASI-PERIODIC HAMILTONIAN SYSTEMS

ÁLVARO FERNÁNDEZ-MORA, ALEX HARO, AND J.M. MONDELO

ABSTRACT. The aim of this paper is to present a method to compute parameterizations of partially hyperbolic invariant tori and their invariant bundles in non-autonomous quasi-periodic Hamiltonian systems. We generalize flow map parameterization methods to the quasi-periodic setting. To this end, we introduce the notion of fiberwise isotropic tori and sketch definitions and results on fiberwise symplectic deformations and their moment maps. These constructs are vital to work in a suitable setting and lead to the proofs of "magic cancellations" that guarantee the existence of solutions of cohomological equations. We apply our algorithms in the Elliptic Restricted Three Body Problem and compute non-resonant 3-dimensional invariant tori and their invariant bundles around the L_1 point.

1. INTRODUCTION

The study of invariant manifolds constitutes the center piece in understanding dynamical systems. It is a rather natural first approach —and often the only hope— to unveil the qualitative behavior of a time-evolving system. Besides the intrinsic interest of invariant manifolds, such structures have found their "real-world" analogues in celestial mechanics, astrodynamics and mission design, plasma physics, semi-classical quantum theory, magnetohydrodynamics, neuroscience, and the list goes on. In particular, celestial mechanics has a long-held tradition in considering such objects, especially periodic orbits and invariant tori carrying quasi-periodic motion, and is in fact one of the main fields that promoted their rigorous and numerical study. Astronomers have used perturbative techniques for centuries in the form of formal series of dubious convergence due to the existence of the so-called small divisors problems. Progress had to wait until the pioneering works [Kol54, Arn63, Mos62] that gave birth to the celebrated KAM theory and the subsequent proofs on the persistence of invariant tori under small enough perturbations of integrable systems.

In later works, KAM theory was carried out far from the perturbative regime, without the need of action-angle variables [dlLGJV05], and rigorous results and algorithms were developed for hyperbolic invariant tori and their whiskers [HdlL06a, HdlL06b, HdlL07]. The methodology is based on the solution of functional equations in the spirit of the parametrization method introduced in [CFdlL03a, CFdlL03b, CFdlL05] for invariant manifolds of fixed points. For the solution of the functional equations, the parameterization method constructs a Newton-like sequence of functions in a scale of Banach spaces that converges to the solution starting from an initial approximation. The results are stated following a posteriori formulation: if there is an approximate solution of the invariance equation satisfying some non-degeneracy conditions, then there exist a true solution nearby. Rather rapidly, the parameterization method lead to a plethora of rigorous results [CCdlL13, CH17b, FdlLS09, GHdlL14, HdlLS12, LV11] and numerical explorations [CCGdlL22, CCH21, CH17a, GHdlL22, HM21, KAdlL22], in different contexts, to name a few. See [HCF$^+$16] for a survey.

Our objective is to design a flow map parameterization method in the spirit of [HM21] to compute non-resonant partially hyperbolic invariant tori and their invariant bundles in quasi-periodic Hamiltonian systems. Time-dependent Hamiltonians appear naturally in astrodynamics and celestial mechanics as improvements of the Circular Restricted Three Body Problem (CRTBP). There is a hierarchy of models of increasing complexity that provide a closer behavior to the real solar system dynamics, which is generally accepted to be given by the Newtonian attraction of the celestial bodies described according to the JPL ephemeris [DTT17]. The improvements of the CRTBP include the Elliptic Restricted Three Body Problem, the Quasi Bicircular problem in the thesis of [And98], and the frequency models of [GMM02], to mention a few. These improved models enable the consideration of advanced space missions concepts and can serve as a seed to compute bounded motion for several decades in the JPL ephemeris model [AS99, And03]. The application of the parameterization method ideas to non-autonomous complex models in astrodynamics and celestial mechanics is our main motivation.

Flow maps methods allow the reduction of the torus dimension to be computed by one [GM01, HM21]. The operation count to manipulate functions grows exponentially with the number of variables of the parameterization. Therefore, the reduction allowed by flow map methods is computationally advantageous. This comes at the expense of numerical integration, which can be easily parallelized. A similar argument can be made for using the parameterization method instead of following a normal form approach. Normal forms require to manipulate functions of the same number of variables as the dimension of the phase space. Instead, the parameterization method requires to manipulate functions with as many variables as the dimension of the invariant manifold. The parameterization method leads to very efficient algorithms. If the parameterization is approximated with either N sample values in a regular grid or N Fourier coefficients, the Newton-like step requires $\mathcal{O}(N)$ storage and $\mathcal{O}(N \log N)$ operations.

This efficiency comes from the geometrical properties of the phase space (i.e. symplectic geometry), the systems (i.e. exact symplecticity), the tori (i.e. isotropy, Lagrangianity), as well as from dynamical properties (i.e. reducibility). In particular, the reducibility of the linearized dynamics around the torus to a block triangular matrix is commonly known as automatic reducibility and it is an important property both in theory [CCdlL13, CH14, dlLGJV05, FdlLS09, GHdlL14, HdlL06a, HdlL06b, HdlLS12, LV11] and applications [CCGdlL22, HM21, KAdlL22]. All these properties lead to the presence of "magic cancellations" and allow the solution of the so-called small divisors equations, which appear naturally in the algorithm and are the hallmark of KAM theory. Proving these cancellations in our context has required the introduction of new geometrical constructs such as fiberwise symplectic deformations. The technical details can be found in the appendices.

Finally, a standard practice when working with non-autonomous systems is to consider an extended phase space by defining extra angle variables and conjugated fictitious variables to make the system autonomous. Although this is mathematically equivalent, this incurs in increasing the dimension of the phase space which leads to less efficient algorithms. We avoid this practice by considering appropriate functional equations. Another standard practice to deal with non-autonomous systems, in particular periodic, is to use flow map methods for a time-T map that make the discrete system autonomous, i.e., choosing for T the period of the system. Instead, we take T as one of the internal periods of the torus sought for. This enables continuation from an autonomous approximation of quasi-periodic models starting directly from tori of the autonomous approximation computed via flow map methods.

Summary of the paper. We provide a full description of the flow map parameterization method for the computation of partially hyperbolic invariant tori and their invariant bundles in non-autonomous quasi-periodic Hamiltonian systems. Section 2 provides the geometrical setting for invariant tori in time-dependent Hamiltonian systems. Section 3 describes the Newton method for computing parameterizations, including the construction of symplectic adapted frames, and a strategy for continuation of the invariant tori with respect to parameters. Section 4 is devoted to the results from the numerical application of the methodology to the Sun-Earth Elliptic Restricted Three Body Problem for 3-dimensional partially hyperbolic invariant tori and their invariant bundles around the L_1 point. Section 5, presents our conclusions.

As mentioned, the appendices contain the proofs that justify our constructions. Appendix A is dedicated to the proof of the smallness of some averages, that are crucial for our algorithms, due to some "magic cancellations" mentioned above. Appendix B introduces the notions of fiberwise symplectic deformations and moment maps which are necessary for the proofs presented in Appendix C for some vanishing averages that are needed in continuation of invariant tori with respect to parameters.

2. Setting

We assume all objects to be sufficiently smooth, even real analytic.

2.1. Hamiltonian systems.

Let us assume we have an *exact symplectic form* $\boldsymbol{\omega}$ on an open set $U \subset \mathbb{R}^{2n}$ endowing U with an exact symplectic structure and let $\Omega : U \to \mathbb{R}^{2n\times 2n}$ be the matrix representation of $\boldsymbol{\omega}$. Let us also assume we have a smooth function $H : U\times\mathbb{R} \to \mathbb{R}$ on the extended phase space that depends explicitly on time. Since the symplectic form is bilinear and non-degenerate, $\boldsymbol{\omega}$ sets a fiberwise linear isomorphism between 1-forms and vector fields. Therefore, there is a unique vector field $X_H : U \times \mathbb{R} \to \mathbb{R}^{2n}$ obtained from the differential of the Hamiltonian as

$$\dot{z} = X_H(z,t) := \Omega(z)^{-1}\mathrm{D}_z H(z,t)^\top, \tag{1}$$

where X_H is the *Hamiltonian vector field* of the *non-autonomous Hamiltonian system* generated by H.

In the present work, we focus on a subset of time-dependent Hamiltonians that frequently arise in physical models such as those in celestial mechanics. We will consider the quasi-periodic case where the time-dependent Hamiltonian is a quasi-periodic function with frequencies $\hat{\alpha} \in \mathbb{R}^\ell$—including the case $\ell = 1$ for which the Hamiltonian is periodic. Later on, further non-resonant conditions will be required for $\hat{\alpha}$. Let $\mathbb{T}^\ell = \mathbb{R}^\ell/\mathbb{Z}^\ell$ be the standard ℓ-torus. We can define the angle variables $\varphi := \hat{\alpha}t \in \mathbb{T}^\ell$, and with a slight abuse of notation, we consider the Hamiltonian as a quasi-periodic smooth function $H : U \times \mathbb{T}^\ell \to \mathbb{R}$. Analogously, we consider the corresponding Hamiltonain vector field $X_H : U \times \mathbb{T}^\ell \to \mathbb{R}^{2n}$. Then, on the extended phase space, we have the following vector field $\tilde{X}_H : U \times \mathbb{T}^\ell \to \mathbb{R}^{2n} \times \mathbb{R}^\ell$ constructed as

$$\begin{pmatrix} \dot{z} \\ \dot{\varphi} \end{pmatrix} = \tilde{X}_H(z,\varphi) = \begin{pmatrix} X_H(z,\varphi) \\ \hat{\alpha} \end{pmatrix}. \tag{2}$$

We look at $\tilde{X}_H$ as a quasi-periodic vector field defined on the total space $U \times \mathbb{T}^\ell$ of a bundle with base $\mathbb{T}^\ell$. On each fiber $\mathcal{F}_\varphi = \pi^{-1}(\varphi)$, where π is the bundle projection, we have a symplectic vector structure and a Hamiltonian vector field $X_H(\cdot,\varphi) : U \to \mathbb{R}^{2n}$. Note that all these vector fields are coupled by the phase equation $\dot{\varphi} = \hat{\alpha}$ according to (2). The vector field $\tilde{X}_H$ is then a fiberwise Hamiltonian vector field—we will see our objects inherit this fiberwise structure in different contexts.

We denote the flow associated to $\tilde{X}_H$ by $\tilde{\phi} : D \subset \mathbb{R}\times U\times\mathbb{T}^\ell \to U\times\mathbb{T}^\ell$, where D is the open set domain of definition of the flow. Then, for every (z, φ), we have the maximal interval of existence $I_{z,\varphi}$ such that the domain of the flow can be expressed as

$$D = \{(t, z, \varphi) \in \mathbb{R} \times U \times \mathbb{T}^\ell \mid t \in I_{z,\varphi}\}.$$

The flow adopts the form

$$\tilde{\phi}(t, z, \varphi) = \begin{pmatrix} \phi(t, z, \varphi) \\ \varphi + \hat{\alpha} t \end{pmatrix}, \tag{3}$$

where the evolution operator ϕ satisfies

$$\frac{\partial \phi}{\partial t}(t, z, \varphi) = X_H\big(\phi(t, z, \varphi), \varphi + \hat{\alpha} t\big), \quad \phi(0, z, \varphi) = z.$$

From now on, we will adopt the standard notations

$$\tilde{\phi}(t, z, \varphi) = \tilde{\phi}_t(z, \varphi), \quad \phi(t, z, \varphi) = \phi_t(z, \varphi).$$

Since $\boldsymbol{\omega}$ is exact, the matrix representation of the 2-form is given by

$$\Omega(z) = \mathrm{D}a(z)^\top - \mathrm{D}a(z), \tag{4}$$

where $a : U \to \mathbb{R}^{2n}$ and $a(z)^\top$ is the matrix representation at $z \in U$ of the *action form* $\boldsymbol{\alpha}$ defined on U. For fixed t, ϕ_t is fiberwise exact symplectic: for each $\varphi \in \mathbb{T}^\ell$, ϕ_t satisfies symplecticity,

$$\mathrm{D}_z\phi_t(z, \varphi)^\top \Omega\big(\phi_t(z, \varphi)\big) \mathrm{D}_z\phi_t(z, \varphi) = \Omega(z), \tag{5}$$

and exactness,

$$\mathrm{D}_z p_t(z, \varphi) = a\big(\phi_t(z, \varphi)\big)^\top \mathrm{D}_z\phi_t(z, \varphi) - a(z)^\top \tag{6}$$

for a *primitive function* $p_t : U \times \mathbb{T}^\ell \to \mathbb{R}$. In particular, this is

$$p_t(z, \varphi) = \int_0^t \Big(a\big(\phi_s(z, \varphi)\big)^\top X_H\big(\phi_s(z, \varphi), \varphi + \hat{\alpha} s\big) - H\big(\phi_s(z, \varphi), \varphi + \hat{\alpha} s\big) \Big)\, ds, \tag{7}$$

which also satisfies

$$\mathrm{D}_\varphi p_t(z, \varphi) = a\big(\phi_t(z, \varphi)\big)^\top \mathrm{D}_\varphi\phi_t(z, \varphi) - \int_0^t \Big(\mathrm{D}_\varphi H\big(\phi_s(z, \varphi), \varphi + \hat{\alpha} s\big)\Big) ds, \tag{8}$$

that we include here for future reference. The existence of the primitive function for the fiberwise exact symplectomorphism ϕ_t allows certain cancellations that are crucial in our iterative scheme for the computation of parameterizations of invariant tori and bundles.

We will also assume we have an almost-complex structure $\boldsymbol{J}$ on U compatible with the symplectic structure, i.e., we have a matrix map $J : U \to \mathbb{R}^{2n\times 2n}$ that is anti-involutive and symplectic; that is

$$J(z)^2 = -I_{2n}, \quad J(z)^\top \Omega(z) J(z) = \Omega(z).$$

The almost-complex structure induces a *Riemannian metric* $\boldsymbol{g}$ with a matrix representation $G : U \to \mathbb{R}^{2n\times 2n}$ defined as $G(z) := -\Omega(z)J(z)$ at each $z \in U$.

Note that we assume the symplectic form to be independent of φ but not constant in U. In the standard case, the symplectic structure, the action form, the almost-complex structure, and the metric adopt the matrix representations

$$\Omega_0(z) = \begin{pmatrix} O_n & -I_n \\ I_n & O_n \end{pmatrix}, \; a_0(z) = \tfrac{1}{2}\begin{pmatrix} O_n & I_n \\ -I_n & O_n \end{pmatrix} z,$$
$$J_0(z) = \begin{pmatrix} O_n & -I_n \\ I_n & O_n \end{pmatrix}, \; G_0(z) = \begin{pmatrix} I_n & O_n \\ O_n & I_n \end{pmatrix}.$$

2.2. **Invariance equations for invariant tori.** We are interested in quasi-periodic solutions for the system given by (2), with frequencies $\hat\omega \in \mathbb{R}^d$ and $\hat\alpha \in \mathbb{R}^\ell$—which correspond to the frequencies of the Hamiltonian. We will refer to $\hat\omega$ and to $\hat\alpha$ as internal and external frequencies, respectively. Geometrically speaking, quasi-periodic solutions lie in $(d+\ell)$-dimensional tori $\tilde{\mathcal{K}} \subset U \times \mathbb{T}^\ell$. In the light of the parameterization method, we consider suitable parameterizations $\tilde K : \mathbb{T}^d \times \mathbb{T}^\ell \to U \times \mathbb{T}^\ell$ that conjugate the dynamics in $\tilde{\mathcal{K}}$ to a linear flow in $\mathbb{T}^d \times \mathbb{T}^\ell$ with frequency $(\hat\omega, \hat\alpha)$. In particular, the frequencies $\hat\omega$ and $\hat\alpha$ need to be, at least, non-resonant or ergodic. That is,

$$k \cdot \hat\omega + j \cdot \hat\alpha \neq 0 \quad \text{for} \quad (k, j) \in \mathbb{Z}^d \times \mathbb{Z}^\ell \setminus \{0\},$$

where $\cdot$ is the standard scalar product. Then, for the range of $\tilde K$ to be an invariant torus, the parameterization is required to satisfy the functional equation

$$\tilde\phi_t \circ \tilde K(\hat\theta, \varphi) - \tilde K(\hat\theta + \hat\omega t, \varphi + \hat\alpha t) = 0, \tag{9}$$

where $\hat\theta \in \mathbb{T}^d, \varphi \in \mathbb{T}^\ell$, and $t \in \mathbb{R}$.

Remark 2.1. *By differentiating* (9) *with respect to t, we obtain the following vector field version of the invariance equation*

$$\tilde X_H \circ \tilde K(\hat\theta, \varphi) = \mathrm{D}_{\hat\theta} \tilde K(\hat\theta, \varphi)\hat\omega + \mathrm{D}_\varphi \tilde K(\hat\theta, \varphi)\hat\alpha.$$

Recall that the extended phase space, $U \times \mathbb{T}^\ell$, has a bundle structure with $\mathbb{T}^\ell$ as the base space. Because of this bundle structure, we consider parameterizations for $\tilde{\mathcal{K}}$ of the form

$$\tilde K(\hat\theta, \varphi) = \begin{pmatrix} \hat K(\hat\theta, \varphi) \\ \varphi \end{pmatrix}, \tag{10}$$

where $\hat{K} : \mathbb{T}^d \times \mathbb{T}^\ell \to U$ parameterizes a $(d+\ell)-$dimensional invariant torus $\hat{\mathcal{K}} \subset U$. Then, for $\tilde{K}$ to satisfy (9), it suffices that $\hat{K}$ satisfies the invariance equation

$$\phi_t\big(\hat{K}(\hat{\theta}, \varphi), \varphi\big) - \hat{K}(\hat{\theta} + \hat{\omega} t, \varphi + \hat{\alpha} t) = 0. \tag{11}$$

From a computational point of view, the cost to compute parameterizations rapidly increases with the dimension of the torus. We therefore follow the trick from [GM01, HM21] and look for a parameterization $K : \mathbb{T}^{d-1} \times \mathbb{T}^\ell \to U$ of a $(d+\ell-1)$-dimensional torus $\mathcal{K} \subset \hat{\mathcal{K}}$, invariant under time-$T$ maps where T is the period associated to one of the internal frequencies of $\hat{\mathcal{K}}$. Note that if the frequencies $\hat{\omega}$ are fixed, then so is T.

Let us first define $\hat{\omega} =: \frac{1}{T}(\omega, 1)$ and $\hat{\alpha} =: \frac{1}{T}\alpha$, where $\omega \in \mathbb{R}^{d-1}$ and $\alpha \in \mathbb{R}^\ell$. In what follows, we will require of (ω, α) stronger non-resonance conditions. We will assume (ω, α) to be Diophantine, meaning that there exists $\gamma > 0$ and $\tau \geq d + \ell - 1$ such that for all $n \in \mathbb{Z}$

$$|k \cdot \omega + j \cdot \alpha - n| \geq \frac{\gamma}{(|k|_1 + |j|_1)^\tau} \quad \text{for} \quad (k, j) \in \mathbb{Z}^{d-1} \times \mathbb{Z}^\ell \setminus \{0\},$$

where $|\cdot|_1$ is the ℓ^1-norm. See Remark 2.7.

We can then assume $\hat{\theta} = (\theta, \theta_d)$, for some fixed $\theta_d \in \mathbb{T}$ and with $\theta \in \mathbb{T}^{d-1}$, and consider a parameterization for $\mathcal{K}$ of the form $K(\theta, \varphi) = \hat{K}(\theta, \theta_d, \varphi)$. If we look at the invariance equation (11) for $t = T$ and some fixed θ_d, we observe that

$$\phi_T\big(\hat{K}(\theta, \theta_d, \varphi), \varphi\big) - \hat{K}(\theta + \omega, \theta_d + 1, \varphi + \alpha) = 0,$$

from where we obtain the following invariance equation for K

$$\phi_T\big(K(\theta, \varphi), \varphi\big) - K(\theta + \omega, \varphi + \alpha) = 0. \tag{12}$$

We refer to ω and α as the internal and external rotation vectors, respectively. We can recover a parameterization for $\hat{\mathcal{K}}$, and consequently for $\tilde{\mathcal{K}}$, from the parameterization of $\mathcal{K}$ as

$$\hat{K}(\hat{\theta}, \varphi) = \phi_{\theta_d T}\big(K(\theta - \theta_d \omega, \varphi - \theta_d \alpha), \varphi - \theta_d \alpha\big). \tag{13}$$

In what follows, we refer to $\mathcal{K}$ as the generator of $\hat{\mathcal{K}}$ and to T as the flying time of $\mathcal{K}$. We emphasize that, although we began by considering a $(d+\ell)-$dimensional invariant torus $\tilde{\mathcal{K}}$ living in the extended phase space $U \times \mathbb{T}^\ell$, this torus is completely determined by $(d+\ell-1)-$dimensional tori $\mathcal{K}$ living in U. Consequently, with this formulation, we not only manage to reduce the dimension of the phase space but also of the invariant tori to be computed.

Remark 2.2. *The parameterizations $\hat{K}$ and K are unique up to rotations and up to unimodular transformations on $\hat{\omega}$ and ω, respectively.*

Remark 2.3. *When the Hamiltonian is periodic with period T_H, it is somewhat standard to look for invariant tori under time-T_H maps, see e.g.* [CJ00]. *Let us illustrate our motivation for taking time$-T$ maps, where T is the period associated to one of the internal frequencies, with a simple example commonly found in applications. Assume we have a T_H-periodic Hamiltonian of the following form,*

$$H(z, \varphi) = H_0(z) + \varepsilon H_1(z, \varphi),$$

where $\varepsilon \in \mathbb{R}$ is some parameter not necessarily small. Also assume that we have computed a parameterization $K_0 : \mathbb{T}^{d-1} \to U$ of a $(d-1)$-dimensional generating torus for the autonomous system given by H_0. It is then natural to consider a parameterization $K_\varepsilon : \mathbb{T}^{d-1} \times \mathbb{T} \to U$ of a d-dimensional generating torus for the system given by H that can be obtained from K_0 by continuation methods in ε. If we take time-T maps where T is the period associated to one of the frequencies of the torus parameterized by K_0, we can construct K_ε at $\varepsilon = 0$ as

$$K_\varepsilon(\theta, \varphi) = K_0(\theta), \tag{14}$$

from where we can directly start the continuation in ε. See Section 3.3. The same argument also holds for the quasi-periodic case.

2.3. **Invariant bundles of rank 1.** In the present work, we focus on $(d + \ell)$-dimensional partially hyperbolic invariant tori with $d = n - 1$. Our choice is motivated by applications such as quasi-periodic perturbations of the Restricted Three Body Problem—this will be the test case explored in Section 4. The results can easily be adapted for Lagrangian tori ($d = n$) and for the lower dimensional case ($d < n-1$). In the later case, a complication is that partially hyperbolic invariant tori are not necessarily reducible. Nonetheless, there exist strategies [HdlL06a, HdlL07, HdlLS12]. Following the results from Section 2.2, we will directly consider rank 1 bundles of $\hat{\mathcal{K}}$ and $\mathcal{K}$ instead of bundles of $\tilde{\mathcal{K}}$.

Let us first consider bundles of rank 1, $\hat{\mathcal{W}}$, with base $\hat{\mathcal{K}}$, invariant under the linearization of ϕ_t on $\hat{\mathcal{K}}$, where the dynamics on the fibers is contracting or expanding. We then look for a parameterization $\hat{W} : \mathbb{T}^d \times \mathbb{T}^\ell \to \mathbb{R}^{2n}$ satisfying

$$\mathrm{D}_z\phi_t\big(\hat{K}(\hat{\theta}, \varphi), \varphi\big)\hat{W}(\hat{\theta}, \varphi) = e^{t\chi}\hat{W}(\hat{\theta} + \hat{\omega}t, \varphi + \hat{\alpha}t), \tag{15}$$

with $\chi \in \mathbb{R}$. If $\chi < 0$, $\hat{\mathcal{W}} = \hat{\mathcal{W}}^s$ is the stable bundle and if $\chi > 0$, $\hat{\mathcal{W}} = \hat{\mathcal{W}}^u$ is the unstable bundle.

We again reduce the dimension of the object by using time$-T$ maps and look for a parameterization $W : \mathbb{T}^{d-1} \times \mathbb{T}^\ell \to \mathbb{R}^{2n}$ of a bundle $\mathcal{W}$ with base $\mathcal{K}$ satisfying

$$\mathrm{D}_z\phi_T\big(K(\theta, \varphi), \varphi\big)W(\theta, \varphi) = W(\theta + \omega, \varphi + \alpha)\lambda, \tag{16}$$

with $\lambda = e^{T\chi}$. We can recover the parameterization of the bundle $\hat{\mathcal{W}}$ as

$$\hat{W}(\hat{\theta}, \varphi) = e^{-\theta_d T\chi} \mathrm{D}_z\phi_{\theta_d T}(K(\theta-\theta_d\omega, \varphi-\theta_d\alpha), \varphi-\theta_d\alpha) W(\theta-\theta_d\omega, \varphi-\theta_d\alpha).$$

Note that because $\hat{\mathcal{W}}$ and $\mathcal{W}$ have rank 1, the dynamics on the fibers is a uniform contraction when $\lambda < 1$ and a uniform expansion when $\lambda > 1$. We will also refer to $\mathcal{W}$ as the generator of $\hat{\mathcal{W}}$, to λ as the Floquet multiplier of $\mathcal{K}$, and to χ as the Floquet exponent of $\hat{\mathcal{K}}$.

Remark 2.4. *Rank 1 stable and unstable bundles are reducible (to constant λ). In general, one could consider rank m stable and unstable bundles that might not be reducible* [HdlL06a, HdlL07, HdlLS12].

Remark 2.5. *We are implicitly assuming the bundles are trivial or that can be trivialized (e.g., by using the double covering trick* [HdlL07]*).*

Remark 2.6. *The invariant bundle $\hat{\mathcal{W}}$, and analogously $\mathcal{W}$, is the linearization on $\hat{\mathcal{K}}$ of certain manifolds $\widehat{\mathcal{W}}$ defined on the annulus: the whiskers. If $\widehat{W} : \mathbb{T}^d \times \mathbb{T}^\ell \times \mathbb{R} \to U$ is a parameterization of a whisker, then it satisfies the invariance equation*

$$\phi_t\big(\widehat{W}(\hat{\theta}, \varphi, s), \varphi\big) = \widehat{W}(\hat{\theta} + \hat{\omega}t, \varphi + \hat{\alpha}t, e^{t\chi}s),$$

where $s \in \mathbb{R}$. Also note that at $s = 0$, $\widehat{W}(\hat{\theta}, \varphi, 0) = \hat{K}(\hat{\theta}, \varphi)$.

2.4. **Geometric properties of invariant tori.** Until now, we have only considered the geometric properties of the phase space. Nevertheless, invariant tori of exact symplectic maps under non-resonance conditions carry certain geometric properties that are of vital importance in our constructions.

For each φ, let us consider tori $\mathcal{K}_\varphi \subset \mathcal{K}$ with parameterizations $K_\varphi : \mathbb{T}^{d-1} \to U$ constructed as $K_\varphi(\theta) = K(\theta, \varphi)$. If we think of $U \times \mathbb{T}^\ell$ as the total space of a bundle with base $\mathbb{T}^\ell$ and projection π, each fiber $\mathcal{F}_\varphi = \pi^{-1}(\varphi)$ contains the torus $\mathcal{K}_\varphi$, see Fig. 1 for a sketch. We will use the same constructions and notation for $\hat{\mathcal{K}}_\varphi \subset \hat{\mathcal{K}}$ and its parameterization $\hat{K}_\varphi$.

Notice that, by differentiating Eq. (12) with respect to θ, we obtain

$$\mathrm{D}_z\phi_T\big(K(\theta, \varphi), \varphi\big)\mathrm{D}_\theta K(\theta, \varphi) = \mathrm{D}_\theta K(\theta + \omega, \varphi + \alpha). \tag{17}$$

We rephrase (17) by saying that the tangent bundle of $\mathcal{K}_\varphi$, parameterized by the column vectors of $\mathrm{D}_\theta K_\varphi$, is transported by the differential $\mathrm{D}_z\phi_T$ as:

$$\mathrm{D}_z\phi_T\big(K_\varphi(\theta), \varphi\big)\mathrm{D}_\theta K_\varphi(\theta) = \mathrm{D}_\theta K_{\varphi+\alpha}(\theta + \omega).$$

From standard arguments, ergodicity of the flow on the torus implies that $\mathcal{K}_\varphi$ is an isotropic torus for each φ, that is, $K_\varphi^*\boldsymbol{\omega} = 0$. In coordinates, this property reads

$$\mathrm{D}_\theta K_\varphi(\theta)^\top \Omega\big(K_\varphi(\theta)\big)\mathrm{D}_\theta K_\varphi(\theta) = 0.$$

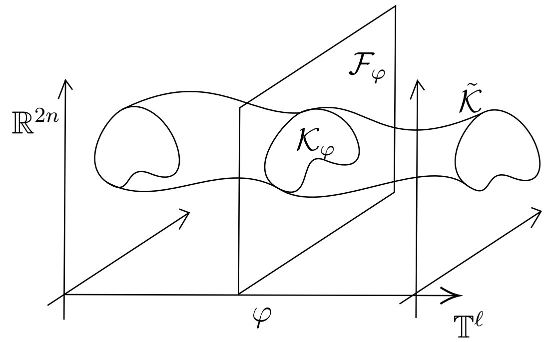

FIGURE 1. Sketch of the torus $\mathcal{K}_\varphi$ within the torus $\tilde{\mathcal{K}}$.

Hence, we think of $\mathcal{K}$ as a φ-parameterized family of $(d-1)$-dimensional isotropic tori and we say that $\mathcal{K}$ is fiberwise isotropic.

As we will see in Section 3.1, because of the invariance of $\mathcal{K}$ and $\mathcal{W}$ and the fiberwise isotropy of $\mathcal{K}$, there exists a set of coordinates given by a symplectic frame that reduces the linearized dynamics to upper triangular form constant along the diagonal. The reducibility of the linearized dynamics allows the efficient computation of invariant tori and bundles and is a property known as *automatic reducibility* in a variety of contexts.

2.5. **Cohomological equations.** In our iterative scheme we will encounter cohomological equations. We dedicate this section to such equations that frequently appear in KAM theory. The material presented here is rather standard, see e.g. [dlL01, Rüs76], but we adapted the formulation to be better suited for our purposes.

In what follows, for functions $\zeta : \mathbb{T}^{d-1} \times \mathbb{T}^\ell \to \mathbb{R}$, that are 1-periodic in each variable, we will often consider their Fourier series

$$\zeta(\theta, \varphi) = \sum_{k \in \mathbb{Z}^{d-1}} \sum_{j \in \mathbb{Z}^\ell} \hat{\zeta}_{kj} \mathrm{e}^{\boldsymbol{i} 2\pi (k\theta + j\varphi)},$$

where $k\theta := \sum_{u=1}^{d-1} k_u \theta_u$, $j\varphi := \sum_{v=1}^{\ell} j_v \varphi_v$, and $\boldsymbol{i}$ is the imaginary unit. Their average is the zero term

$$\hat{\zeta}_{00} = \langle \zeta \rangle := \iint_{\mathbb{T}^{d-1} \times \mathbb{T}^\ell} \zeta(\theta, \varphi)\, d\theta\, d\varphi.$$

2.5.1. *Non-small divisors cohomological equations.* Let $\xi, \eta : \mathbb{T}^{d-1} \times \mathbb{T}^\ell \to \mathbb{R}$ be analytic functions and let $\omega \in \mathbb{R}^{d-1}$ and $\alpha \in \mathbb{R}^\ell$ be fixed rotation vectors. For ease of notation, let us define $\bar{\theta} := \theta + \omega$ and $\bar{\varphi} := \varphi + \alpha$.

We first consider functional equations of the form

$$\lambda \xi(\theta, \varphi) - \mu \xi(\bar{\theta}, \bar{\varphi}) = \eta(\theta, \varphi), \tag{18}$$

with $\lambda, \mu \in \mathbb{R}$ such that $|\lambda| \neq |\mu|$ and where η, ω, and α are known and ξ is to be found. If we express ξ and η as Fourier series

$$\xi(\theta,\varphi) = \sum_{k\in\mathbb{Z}^{d-1}} \sum_{j\in\mathbb{Z}^{\ell}} \hat{\xi}_{kj} \mathrm{e}^{\boldsymbol{i}2\pi(k\theta+j\varphi)}, \quad \eta(\theta,\varphi) = \sum_{k\in\mathbb{Z}^{d-1}} \sum_{j\in\mathbb{Z}^{\ell}} \hat{\eta}_{kj} \mathrm{e}^{\boldsymbol{i}2\pi(k\theta+j\varphi)},$$

the solution of (18) is formally given by

$$\hat{\xi}_{kj} = \frac{\hat{\eta}_{kj}}{\lambda - \mu \mathrm{e}^{\boldsymbol{i}2\pi(k\omega+j\alpha)}} \quad \forall k, j.$$

2.5.2. *Small-divisors cohomological equations.* We will also consider functional equations of the form

$$\xi(\theta,\varphi) - \xi(\bar{\theta},\bar{\varphi}) = \eta(\theta,\varphi), \tag{19}$$

where η, ω, and α are known and ξ is to be found. If $\langle\eta\rangle = 0$, the solution of (19) is formally given by

$$\begin{aligned} \hat{\xi}_{00} &\in \mathbb{R} \quad \text{free}, \\ \hat{\xi}_{kj} &= \frac{\hat{\eta}_{kj}}{1 - \mathrm{e}^{\boldsymbol{i}2\pi(k\omega+j\alpha)}} \quad \text{for } k, j \neq 0. \end{aligned}$$

Remark 2.7. *Note that $1 - \mathrm{e}^{\boldsymbol{i}2\pi(k\omega+j\alpha)}$ can become arbitrarily small even if ω and α are non-resonant—this is the so called* small divisors problem*. For analytic η, the convergence of the series for ξ is guaranteed by requiring stronger non-resonant conditions—that is, the Diophantine condition. This is standard in KAM theory*

3. Flow map parameterization methods

In this section we develop the methodology for computing parameterizations of generating tori $\mathcal{K}$ and generating bundles $\mathcal{W}$ for $(d+\ell)$-dimensional partially hyperbolic invariant tori $\hat{\mathcal{K}}$ and their invariant bundles $\hat{\mathcal{W}}$, respectively, where $d = n-1$.

3.1. **Adapted frames.** We proceed to construct symplectic frames $P : \mathbb{T}^{d-1} \times \mathbb{T}^{\ell} \to \mathbb{R}^{2n\times 2n}$ in order to leverage the automatic reducibility of the tori. We look for a vector bundle map over the identity such that, in suitable coordinates, the linear dynamics reduce to an upper triangular matrix as

$$P(\bar{\theta},\bar{\varphi})^{-1} \mathrm{D}_z\phi_T\big(K(\theta,\varphi),\varphi\big) P(\theta,\varphi) = \left(\begin{array}{c|c} \Lambda & S(\theta,\varphi) \\ \hline O_n & \Lambda^{-\top} \end{array}\right), \tag{20}$$

with

$$\Lambda = \begin{pmatrix} I_{n-1} & 0 \\ 0 & \lambda \end{pmatrix}, \quad S(\theta,\varphi) = \begin{pmatrix} S^1(\theta,\varphi) & 0 \\ 0 & 0 \end{pmatrix}, \tag{21}$$

where each 0 block corresponds to a zero matrix of suitable dimensions and S^1 is the $(n-1)\times(n-1)$ symmetric matrix known as the torsion matrix.

The construction of the frame P follows from first constructing a subframe $L : \mathbb{T}^{d-1} \times \mathbb{T}^{\ell} \to \mathbb{R}^{2n\times n}$ that is invariant under the differential of time-T maps on $\mathcal{K}$; that is, L is required to satisfy

$$\mathrm{D}_z\phi_T\big(K(\theta,\varphi),\varphi\big)L(\theta,\varphi) = L(\bar\theta,\bar\varphi)\Lambda. \tag{22}$$

Note that this is a necessary condition for the frame P to satisfy (20). Also, according to (17) and (16), $\mathrm{D}_\theta K$ and W are invariant under the differential of time-T maps and they are therefore suitable to partly generate the subframe L. For autonomous Hamiltonian systems, the Hamiltonian vector field is invariant under the differential of time-T maps and, consequently, this suffices to construct the subframe L, see [HM21]. For periodic and quasi-periodic Hamiltonians, this is no longer the case due to the time dependency. We need to construct a new object invariant under $\mathrm{D}_z\phi_T$—this is the key element to apply the same ideas of flow map parameterization methods for autonomous systems to our setting.

Let us first derive Eq. (12) with respect to φ to obtain

$$\mathrm{D}_z\phi_T\big(K(\theta,\varphi),\varphi\big)\mathrm{D}_\varphi K(\theta,\varphi) + \mathrm{D}_\varphi\phi_T\big(K(\theta,\varphi),\varphi\big) = \mathrm{D}_\varphi K(\bar\theta,\bar\varphi). \tag{23}$$

For the flow $\tilde\phi$, let us consider

$$\tfrac{d}{dt}\tilde\phi_T \circ \tilde\phi_t(z,\varphi) \tag{24}$$

at $t = 0$ and observe that we have the identity

$$\begin{pmatrix} \mathrm{D}_z\phi_T(z,\varphi) & \mathrm{D}_\varphi\phi_T(z,\varphi) \\ O_{\ell\times 2n} & I_\ell \end{pmatrix} \begin{pmatrix} X_H(z,\varphi) \\ \hat\alpha \end{pmatrix} = \begin{pmatrix} X_H\big(\phi_T(z,\varphi),\bar\varphi\big) \\ \hat\alpha \end{pmatrix}. \tag{25}$$

Then, using (23) and evaluating (25) on the torus, i.e., at $z = K(\theta,\varphi)$, it is easy to show that

$$\mathrm{D}_z\phi_T\big(K(\theta,\varphi),\varphi\big)\mathcal{X}_H(\theta,\varphi) = \mathcal{X}_H(\bar\theta,\bar\varphi), \tag{26}$$

where

$$\mathcal{X}_H(\theta,\varphi) := X_H\big(K(\theta,\varphi),\varphi\big) - \mathrm{D}_\varphi K(\theta,\varphi)\hat\alpha \tag{27}$$

is a geometric object defined on the torus that is invariant under $\mathrm{D}_z\phi_T$. Additionally, at each (θ,φ), $\mathcal{X}_H(\theta,\varphi)$ complements the column vectors of $\mathrm{D}_\theta K(\theta,\varphi)$, tangent to $\mathcal{K}_\varphi$ at $K(\theta,\varphi)$, to a full basis of the tangent bundle of $\hat{\mathcal{K}}_\varphi$ at $\hat K(\theta,\varphi)$. Such interpretation follows from differentiating (13) with respect to θ_d at $\theta_d = 0$.

From (16),(17), and (26) it is immediate to see that the subframe $L : \mathbb{T}^{d-1} \times \mathbb{T}^{\ell} \to \mathbb{R}^{2n\times n}$, given by

$$L(\theta,\varphi) := \Big(\mathrm{D}_\theta K(\theta,\varphi) \quad \mathcal{X}_H(\theta,\varphi) \quad W(\theta,\varphi)\Big) \tag{28}$$

satisfies (22). Additionally, L has full rank since $\mathrm{D}_\theta K$ and $\mathcal{X}_H$ generate the tangent bundle at $\mathcal{K}_\varphi$ of the $(n-1)$-dimensional torus $\hat{\mathcal{K}}_\varphi$ and W generates the stable or the unstable bundle. Following [HCF$^+$16], it can be shown that L is a fiberwise Lagrangian frame. That is, for each $\varphi \in \mathbb{T}^\ell$, $L_\varphi(\theta) := L(\theta, \varphi)$ generates a Lagrangian subspace on $T_{\mathcal{K}_\varphi} U$. In coordinates, this property implies that

$$L(\theta, \varphi)^\top \Omega\big(K(\theta, \varphi)\big) L(\theta, \varphi) = 0. \tag{29}$$

We now proceed to complement the subframe L with a subframe $N : \mathbb{T}^{d-1} \times \mathbb{T}^\ell \to \mathbb{R}^{2n \times n}$ such that the frame P is symplectic with respect to the standard symplectic form. Note that the symplecticity of P implies the subframe N also needs to be fiberwise Lagrangian. There exists several ways to construct the subframe N, see e.g. [HCF+16] for details. We will use the almost complex structure and the Riemannian metric to construct

$$\hat{N}(\theta, \varphi) := J\big(K(\theta, \varphi)\big) L(\theta, \varphi) G_K(\theta, \varphi)^{-1}, \tag{30}$$

$$G_K(\theta, \varphi) := L(\theta, \varphi)^\top G\big(K(\theta, \varphi)\big) L(\theta, \varphi). \tag{31}$$

Then, it follows that the frame $\hat{P}(\theta, \varphi) = \Big(L(\theta, \varphi) | \hat{N}(\theta, \varphi)\Big)$ is symplectic and satisfies

$$\hat{P}(\bar{\theta}, \bar{\varphi})^{-1} \mathrm{D}_z \phi_T\big(K(\theta, \varphi), \varphi\big) \hat{P}(\theta, \varphi) = \left(\begin{array}{c|c} \Lambda & \hat{S}(\theta, \varphi) \\ \hline O_n & \Lambda^{-\top} \end{array}\right), \tag{32}$$

where

$$\hat{S}(\theta, \varphi) = \hat{N}(\bar{\theta}, \bar{\varphi})^\top \Omega\big(K(\bar{\theta}, \bar{\varphi})\big) \mathrm{D}_z \phi_T\big(K(\theta, \varphi), \varphi\big) \hat{N}(\theta, \varphi), \tag{33}$$

and, due to symplecticity, $\hat{S}(\theta, \varphi)\Lambda^\top = \Lambda \hat{S}(\theta, \varphi)^\top$ holds.

Note that the frame $\hat{P}$ does not yet satisfy (20) as the torsion matrix given by $\hat{S}$ needs to be transformed to adopt the reduced form given in (21). In doing so, we get another invariant bundle generated by the last column of P. We construct a new symplectic frame by considering symplectic transformations

$$Q(\theta, \varphi) = \left(\begin{array}{c|c} I_n & B(\theta, \varphi) \\ \hline O_n & I_n \end{array}\right), \tag{34}$$

with B symmetric, such that the frame

$$P(\theta, \varphi) := \hat{P}(\theta, \varphi) Q(\theta, \varphi) \tag{35}$$

satisfies (20). This translates into the matrix

$$S(\theta, \varphi) = \Lambda B(\theta, \varphi) + \hat{S}(\theta, \varphi) - B(\bar{\theta}, \bar{\varphi})\Lambda^{-\top} \tag{36}$$

adopting the required form which, in turn, determines the matrix B. Let us define splittings in blocks of sizes $(n-1) \times (n-1), (n-1) \times 1, 1 \times (n-1)$ and 1×1 for $\hat{S}$ as

$$\hat{S}(\theta, \varphi) = \begin{pmatrix} \hat{S}^1(\theta, \varphi) & \hat{S}^2(\theta, \varphi) \\ \hat{S}^3(\theta, \varphi) & \hat{S}^4(\theta, \varphi) \end{pmatrix}, \tag{37}$$

and define analogous splittings for the matrices S and B. Then, expression (36) reads

$$S^1(\theta,\varphi) = \hat{S}^1(\theta,\varphi) + B^1(\theta,\varphi) \quad - B^1(\bar\theta,\bar\varphi), \tag{38}$$

$$S^2(\theta,\varphi) = \hat{S}^2(\theta,\varphi) + B^2(\theta,\varphi) \quad - B^2(\bar\theta,\bar\varphi)\lambda^{-1}, \tag{39}$$

$$S^3(\theta,\varphi) = \hat{S}^3(\theta,\varphi) + B^3(\theta,\varphi)\lambda - B^3(\bar\theta,\bar\varphi), \tag{40}$$

$$S^4(\theta,\varphi) = \hat{S}^4(\theta,\varphi) + B^4(\theta,\varphi)\lambda - B^4(\bar\theta,\bar\varphi)\lambda^{-1}. \tag{41}$$

We require that $S^3(\theta,\varphi)^\top = S^2(\theta,\varphi) = 0$ and $S^4(\theta,\varphi) = 0$, whereas no restriction is applied to S^1. Consequently, our requirement on the frame P translates into

$$B^2(\theta,\varphi) \quad - B^2(\bar\theta,\bar\varphi)\lambda^{-1} = -\hat{S}^2(\theta,\varphi), \tag{42}$$

$$B^4(\theta,\varphi)\lambda - B^4(\bar\theta,\bar\varphi)\lambda^{-1} = -\hat{S}^4(\theta,\varphi), \tag{43}$$

and $B^3(\theta,\varphi)^\top = B^2(\theta,\varphi)$. We then choose $B^1(\theta,\varphi) = I_{n-1}$, which results in $S^1(\theta,\varphi) = \hat{S}^1(\theta,\varphi)$. Equations (42) and (43) are non-small divisors cohomological equations that can be solved as detailed in Section 2.5. The construction of adapted frames is summarized with the following algorithm.

Algorithm 3.1. *(Computation of adapted frames) Given* (K, W, λ) *satisfying* (12) *and* (16)*, compute the adapted frame* P *and the reduced dynamics by following these steps:*

(1) *Compute* $\mathcal{X}_H(\theta,\varphi)$ *from* (27).
(2) *Compute* $L(\theta,\varphi)$ *from* (28).
(3) *Compute* $\hat{N}(\theta,\varphi)$ *from* (30).
(4) *Compute* $\hat{S}(\theta,\varphi)$ *from* (33)*, let* $B^1(\theta,\varphi) = I_{n-1}$*, and* $S^1(\theta,\varphi) = \hat{S}^1(\theta,\varphi)$.
(5) *Compute* $B^2(\theta,\varphi)$ *by solving* (42) *and let* $B^3(\theta,\varphi) = B^2(\theta,\varphi)^\top$.
(6) *Compute* $B^4(\theta,\varphi)$ *by solving* (43).
(7) *Compute* $P(\theta,\varphi)$ *from* (35) *with* $Q(\theta,\varphi)$ *given by* (34).

3.2. **Description of a Newton step.** Given (K, W, λ) that approximately satisfy equations (12) and (16), our aim is to improve such approximations with an iterative scheme. Let us define the error in the invariance of $\mathcal{K}$ and $\mathcal{W}$ as the functions $E^K, E^W : \mathbb{T}^{d-1} \times \mathbb{T}^\ell \to \mathbb{R}^{2n}$ given by

$$E^K(\theta,\varphi) := \phi_T\big(K(\theta,\varphi),\varphi\big) - K(\bar\theta,\bar\varphi), \tag{44}$$

$$E^W(\theta,\varphi) := \mathrm{D}_z\phi_T\big(K(\theta,\varphi),\varphi\big)W(\theta,\varphi) - W(\bar\theta,\bar\varphi)\lambda. \tag{45}$$

Since $\mathcal{K}$ and $\mathcal{W}$ are approximately invariant, $\mathcal{K}$ is approximately reducible. That is, there is an error in the reducibility of the linearized dynamics controlled by E^K and E^W as

$$P(\bar\theta,\bar\varphi)^{-1}\mathrm{D}_z\phi_T\big(K(\theta,\varphi),\varphi\big)P(\theta,\varphi) = \begin{pmatrix} \Lambda & S(\theta,\varphi) \\ O_n & \Lambda^{-\top} \end{pmatrix} + \mathcal{O}(\|E^K\|, \|E^W\|)$$

for some suitable norms. Also, the matrix P is approximately symplectic. Therefore, instead of computing its inverse, we can use that

$$P(\bar\theta,\bar\varphi)^{-1} = -\Omega_0 P(\bar\theta,\bar\varphi)^\top \Omega\big(K(\bar\theta,\bar\varphi)\big) + \mathcal{O}(\|E^K\|, \|E^W\|)$$

to compute an approximate inverse. Recall that Ω_0 is the standard symplectic form. In order to improve the parameterizations for $\mathcal{K}$ and $\mathcal{W}$, we add corrections to their parameterizations such that the linearized invariance equations vanish at first order. Therefore, we can neglect the error in the reducibility of the linearized dynamics and in the inverse of P as long as their contributions is of second order or higher.

3.2.1. *A Newton step on the torus.* We proceed by adding a correction $\Delta K : \mathbb{T}^{d-1} \times \mathbb{T}^\ell \to \mathbb{R}^{2n}$ to the parameterization K. The invariance equation on the corrected torus then reads

$$\phi_T\big(K(\theta,\varphi) + \Delta K(\theta,\varphi), \varphi\big) - K(\bar\theta,\bar\varphi) - \Delta K(\bar\theta,\bar\varphi) = 0. \tag{46}$$

We linearize the equation around the approximate torus in order to find the correction ΔK that makes equation (46) vanish at first order. Let us use the frame P and write the correction in coordinates such that $\Delta K(\theta,\varphi) = P(\theta,\varphi)\xi(\theta,\varphi)$. Expanding around the approximated torus and retaining only terms up to first order results in

$$\mathrm{D}_z\phi_T\big(K(\theta,\varphi),\varphi\big)P(\theta,\varphi)\xi(\theta,\varphi) - P(\bar\theta,\bar\varphi)\xi(\bar\theta,\bar\varphi) = -E^K(\theta,\varphi). \tag{47}$$

We then left-multiply by $P(\bar\theta,\bar\varphi)^{-1}$ and neglect higher order terms to obtain

$$\begin{pmatrix} \Lambda & S(\theta,\varphi) \\ 0 & \Lambda^{-\top} \end{pmatrix} \xi(\theta,\varphi) - \xi(\bar\theta,\bar\varphi) = \eta(\theta,\varphi), \tag{48}$$

where

$$\eta(\theta,\varphi) = \Omega_0 P(\bar\theta,\bar\varphi)^\top \Omega\big(K(\bar\theta,\bar\varphi)\big) E^K(\theta,\varphi). \tag{49}$$

Let us write ξ and η into $(n-1)\times 1 \times (n-1) \times 1$ components as

$$\xi(\theta,\varphi) = \begin{pmatrix} \xi^1(\theta,\varphi) \\ \xi^2(\theta,\varphi) \\ \xi^3(\theta,\varphi) \\ \xi^4(\theta,\varphi) \end{pmatrix}, \quad \eta(\theta,\varphi) = \begin{pmatrix} \eta^1(\theta,\varphi) \\ \eta^2(\theta,\varphi) \\ \eta^3(\theta,\varphi) \\ \eta^4(\theta,\varphi) \end{pmatrix}.$$

Observing that $\langle \eta^3 \rangle$ is quadratically small—see Appendix A—we neglect again higher order terms to write (48) as

$$\xi^1(\theta,\varphi) + S^1(\theta,\varphi)\xi^3(\theta,\varphi) - \xi^1(\bar\theta,\bar\varphi) = \eta^1(\theta,\varphi), \tag{50}$$

$$\lambda\xi^2(\theta,\varphi) - \xi^2(\bar\theta,\bar\varphi) = \eta^2(\theta,\varphi), \tag{51}$$

$$\xi^3(\theta,\varphi) - \xi^3(\bar\theta,\bar\varphi) = \eta^3(\theta,\varphi) - \langle\eta^3\rangle, \tag{52}$$

$$\lambda^{-1}\xi^4(\theta,\varphi) - \xi^4(\bar\theta,\bar\varphi) = \eta^4(\theta,\varphi), \tag{53}$$

Note that equations (51) and (53) are non-small divisors cohomological equations whereas equation (52) is a small divisors cohomological equation. Once ξ^3 is solved for, equation (50) is also a small divisors cohomological equation. Since (52) is solvable (assuming Diophantine conditions), with $\langle \xi^3 \rangle$ free, we adjust its value in order to adjust averages in (50). That is, we will use this freedom to solve equation (50) as a small divisors cohomological equation. See Section 2.5.

Let us consider

$$\xi^3(\theta,\varphi) = \xi^3_0 + \tilde{\xi}^3(\theta,\varphi),$$

where $\tilde{\xi}^3$, solves (52) with $\langle \tilde{\xi}^3 \rangle = 0$. Then, equation (50) becomes

$$\xi^1(\theta,\varphi) - \xi^1(\bar{\theta},\bar{\varphi}) = \eta^1(\theta,\varphi) - S^1(\theta,\varphi)\tilde{\xi}^3(\theta,\varphi) - S^1(\theta,\varphi)\xi^3_0.$$

We now choose ξ^3_0 such that

$$\langle S^1 \rangle \xi^3_0 = \langle \eta^1 - S^1 \tilde{\xi}^3 \rangle. \tag{54}$$

Hence, we can now solve equation (50) as a small divisors cohomological equation with $\langle \xi^1 \rangle$ free; a simple choice is to take $\langle \xi^1 \rangle = 0$. This underdeterminacy reflects the underdeterminacy of the parameterization of the generating torus $\mathcal{K}$ under phase shifts in $\mathbb{T}^{d-1}$ and translations within $\hat{\mathcal{K}}$, see Remark 2.2. The Newton step on the torus is summarized with the following algorithm.

Algorithm 3.2. *(Newton step on the torus) Let (K, W, λ) satisfy equations* (12) *and* (16) *approximately. Obtain the corrected generating torus by following these steps:*

(1) *Compute $P(\theta,\varphi)$ and $S^1(\theta,\varphi)$ by following Algorithm 3.1.*
(2) *Compute the error $E^K(\theta,\varphi)$ from* (44).
(3) *Compute $\eta(\theta,\varphi)$, the right-hand side of the cohomological equations given in* (48), *from* (49).
(4) *Solve* (51) *and* (53) *as non-small divisors cohomological equations in order to obtain $\xi^2(\theta,\varphi)$ and $\xi^4(\theta,\varphi)$.*
(5) *Solve* (52) *as small divisors cohomological equations in order to obtain its zero-average solution $\tilde{\xi}^3(\theta,\varphi)$.*
(6) *Compute $\langle S^1 \rangle$ and the right-hand side of the linear system* (54) *and solve it in order to obtain ξ^3_0.*
(7) *Solve* (50) *as small divisors cohomological equations in order to obtain $\xi^1(\theta,\varphi)$ with $\langle \xi^1 \rangle = 0$.*
(8) *Set $K(\theta,\varphi) \leftarrow K(\theta,\varphi) + P(\theta,\varphi)\xi(\theta,\varphi)$.*

3.2.2. *A Newton step on the bundle.* Once we have corrected the parameterization of the generating torus in the previous step, we proceed in an analogous manner and add corrections $\Delta W : \mathbb{T}^{d-1} \times \mathbb{T}^{\ell} \to \mathbb{R}^{2n}$ and $\Delta\lambda \in \mathbb{R}$ to the parameterization of the generating bundle and to the Floquet multiplier, respectively. Then, on the corrected bundle, we obtain from (16)

$$\mathrm{D}_z\phi_T\big(K(\theta,\varphi),\varphi\big)\big(W(\theta,\varphi)+\Delta W(\theta,\varphi)\big) - \big(W(\bar{\theta},\bar{\varphi}) + \Delta W(\bar{\theta},\bar{\varphi})\big)\,(\lambda+\Delta\lambda) = 0.$$

We choose the corrections such that the previous equation vanishes at first order. Again, we write the correction term for the bundle in coordinates such that $\Delta W(\theta,\varphi) = P(\theta,\varphi)\xi(\theta,\varphi)$ and expand the previous expression retaining terms up to first order to obtain

$$\mathrm{D}_z\phi_T\big(K(\theta,\varphi),\varphi\big)P(\theta,\varphi)\xi(\theta,\varphi) - P(\bar\theta,\bar\varphi)\xi(\bar\theta,\bar\varphi)\lambda - W(\bar\theta,\bar\varphi)\Delta\lambda = -E^W(\theta,\varphi).$$

We then left-multiply by $P(\bar\theta,\bar\varphi)^{-1}$, use equation (20), and neglect second order terms to obtain

$$\begin{pmatrix} \Lambda & S(\theta,\varphi) \\ O_n & \Lambda^{-\top} \end{pmatrix} \xi(\theta,\varphi) - \lambda\xi(\bar\theta,\bar\varphi) - e_n\Delta\lambda = \eta(\theta,\varphi), \tag{55}$$

with

$$e_n = \begin{pmatrix} 0_{n-1} \\ 1 \\ 0_{n-1} \\ 0 \end{pmatrix},$$

and

$$\eta(\theta,\varphi) = \Omega_0 P(\bar\theta,\bar\varphi)^\top \Omega\big(K(\bar\theta,\bar\varphi)\big)E^W(\theta,\varphi). \tag{56}$$

We can split ξ and η as in the previous section and rewrite (55) as

$$\xi^1(\theta,\varphi) + S^1(\theta,\varphi)\xi^3(\theta,\varphi) - \lambda\xi^1(\bar\theta,\bar\varphi) = \eta^1(\theta,\varphi), \tag{57}$$
$$\lambda\xi^2(\theta,\varphi) - \lambda\xi^2(\bar\theta,\bar\varphi) - \Delta\lambda = \eta^2(\theta,\varphi), \tag{58}$$
$$\xi^3(\theta,\varphi) - \lambda\xi^3(\bar\theta,\bar\varphi) = \eta^3(\theta,\varphi), \tag{59}$$
$$\lambda^{-1}\xi^4(\theta,\varphi) - \lambda\xi^4(\bar\theta,\bar\varphi) = \eta^4(\theta,\varphi). \tag{60}$$

Equations (59) and (60) can be solved as non-small divisors cohomological equations and, once ξ^3 is known, equation (57) can also be solved as a non-small divisors cohomological equation. On the contrary, equation (58) can be solved as a small divisors cohomological equation with $\langle\xi^2\rangle$ free once we adjust the average of the right hand side by taking $\Delta\lambda = -\langle\eta^2\rangle$. The freedom in $\langle\xi^2\rangle$ is related to the freedom in the length of W, analogous to the underdeterminacy of the lengths of eigenvectors in an eigenvalue problem. We then take the simplest choice for this average, i.e., $\langle\xi^2\rangle = 0$. The Newton step on the bundle is summarized with the following algorithm.

Algorithm 3.3. *(Newton step on the bundle) Let (K, W, λ) satisfy equations* (12) *and* (16) *approximately. Obtain the corrected generating bundle and Floquet multiplier by following these steps:*

(1) *Compute $P(\theta,\varphi)$ and $S^1(\theta,\varphi)$ by following Algorithm 3.1.*
(2) *Compute the error $E^W(\theta,\varphi)$ from* (45).
(3) *Compute $\eta(\theta,\varphi)$, the right-hand side of the cohomological equations given in* (55), *from* (56).

(4) *Solve* (59), (60), *and* (57) *as non-small divisors cohomological equations in order to obtain* $\xi^3(\theta,\varphi)$, $\xi^4(\theta,\varphi)$, *and* $\xi^1(\theta,\varphi)$, *respectively.*
(5) *Take* $\Delta\lambda = -\langle \eta^2 \rangle$.
(6) *Solve* (58) *as a small divisors cohomological equation in order to obtain* $\xi^2(\theta,\varphi)$ *with* $\langle \xi^2 \rangle = 0$,
(7) *Set* $W(\theta,\varphi) \leftarrow W(\theta,\varphi) + P(\theta,\varphi)\xi(\theta,\varphi)$ *and* $\lambda \leftarrow \lambda + \Delta\lambda$.

3.3. **Continuation with respect to external parameters.** Let us assume we have a family of Hamiltonians H_ε that depends analytically on some parameter $\varepsilon \in \mathbb{R}$. Given $(K, W, \lambda)_\varepsilon$ for certain value of ε that satisfies equations (12) and (16), we want to compute parameterizations of a generating torus and generating bundle (with the corresponding Floquet multiplier) for a different Hamiltonian $H_{\varepsilon'}$. As commonly done in continuation methods, see e.g. [AG90], we will provide a methodology to compute the tangent to the continuation curve with respect to ε from where we obtain a first order approximation of the invariant objects for $H_{\varepsilon'}$.

Let us assume equations (12) and (16) define implicitly $(K, W, \lambda)_\varepsilon$ as functions of ε. Then, we want to compute $\partial_\varepsilon K, \partial_\varepsilon W$, and $\partial_\varepsilon \lambda$. In the following, for the sake of notation clarity, we will omit the dependency of (K, W, λ) and of ϕ_T on ε. Let us begin by taking Eq. (12) and differentiate it with respect to ε to obtain

$$\mathrm{D}_z\phi_T\big(K(\theta,\varphi),\varphi\big)\partial_\varepsilon K(\theta,\varphi) - \partial_\varepsilon K(\bar\theta,\bar\varphi) + \partial_\varepsilon\phi_T\big(K(\theta,\varphi),\varphi\big) = 0,$$

where $\partial_\varepsilon\phi_T$ is the variation of the map ϕ_T with respect to ε that can be computed through variational equations. We now express the derivatives in the frame such that $\partial_\varepsilon K(\theta,\varphi) = P(\theta,\varphi)\xi(\theta,\varphi)$. The previous expression then reads

$$\mathrm{D}_z\phi_T\big(K(\theta,\varphi),\varphi\big)P(\theta,\varphi)\xi(\theta,\varphi) - P(\bar\theta,\bar\varphi)\xi(\bar\theta,\bar\varphi) + \partial_\varepsilon\phi_T\big(K(\theta,\varphi),\varphi\big) = 0$$

and, after left-multiplication by $P(\bar\theta,\bar\varphi)^{-1}$, we have

$$\begin{pmatrix} \Lambda & S(\theta,\varphi) \\ 0 & \Lambda^{-\top} \end{pmatrix} \xi(\theta,\varphi) - \xi(\bar\theta,\bar\varphi) = \eta(\theta,\varphi), \tag{61}$$

where

$$\eta(\theta,\varphi) = \Omega_0 P(\bar\theta,\bar\varphi)^\top \Omega\big(K(\bar\theta,\bar\varphi)\big)\partial_\varepsilon\phi_T\big(K(\theta,\varphi),\varphi\big). \tag{62}$$

The cohomological equations given in (61) can be solved exactly as described in Section 3.2.1 but with η given by (62).

Remark 3.1. *For the system given by* (61) *to be solvable, we encounter again small divisors cohomological equations for* ξ^3 *(recall the splittings defined in Section 3.2.1) that require* $\langle \eta^3 \rangle = 0$. *Using fiberwise symplectic deformations, see Appendix B, we prove in Appendix C that, for* η *defined as in* (62), $\langle \eta^3 \rangle = 0$.

In order to obtain $\partial_\varepsilon W$ and $\partial_\varepsilon \lambda$, we differentiate equation (16) with respect to ε to obtain

$$\partial_\varepsilon \Big(\mathrm{D}_z \phi_T\big(K(\theta,\varphi),\varphi\big)\Big) W(\theta,\varphi) + \mathrm{D}_z \phi_T\big(K(\theta,\varphi),\varphi\big)\partial_\varepsilon W(\theta,\varphi) - W(\bar\theta,\bar\varphi)\partial_\varepsilon\lambda - \partial_\varepsilon W(\bar\theta,\bar\varphi)\lambda = 0,$$

which can be rewritten as

$$\mathrm{D}_z \phi_T\big(K(\theta,\varphi),\varphi\big)\partial_\varepsilon W(\theta,\varphi) - \partial_\varepsilon W(\bar\theta,\bar\varphi)\lambda - W(\bar\theta,\bar\varphi)\partial_\varepsilon\lambda = -E^{\partial_\varepsilon W}(\theta,\varphi), \tag{63}$$

with

$$\begin{aligned} E^{\partial_\varepsilon W}(\theta,\varphi) &= \partial_\varepsilon \Big(\mathrm{D}_z \phi_T\big(K(\theta,\varphi),\varphi\big)\Big) W(\theta,\varphi) \\ &= \partial_\varepsilon \mathrm{D}_z \phi_T\big(K(\theta,\varphi),\varphi\big) W(\theta,\varphi) + \mathrm{D}^2_z \phi_T\big(K(\theta,\varphi),\varphi\big)[W(\theta,\varphi), \partial_\varepsilon K(\theta,\varphi)]. \end{aligned} \tag{64}$$

The form $\mathrm{D}^2_z \phi_T\big(z,\varphi\big)[\cdot,\cdot]$ is the bilinear form given by the second differential of ϕ_T with respect to z that can be computed through variational equations. Then, by using the frame such that $\partial_\varepsilon W(\theta,\varphi) = P(\theta,\varphi)\xi(\theta,\varphi)$, and after left-multiplication by $P(\bar\theta,\bar\varphi)^{-1}$, expression (63) reads

$$\begin{pmatrix} \Lambda & S(\theta,\varphi) \\ 0 & \Lambda^{-\top} \end{pmatrix} \xi(\theta,\varphi) - \lambda\xi(\bar\theta,\bar\varphi) - e_n \partial_\varepsilon\lambda = \eta(\theta,\varphi), \tag{65}$$

with

$$\eta(\theta,\varphi) = \Omega_0 P(\bar\theta,\bar\varphi)^\top \Omega\big(K(\bar\theta,\bar\varphi)\big) E^{\partial_\varepsilon W}(\theta,\varphi). \tag{66}$$

These cohomological equations can be solved exactly as described in Section 3.2.2 but with η given by (66). The computation of derivatives of (K, W, λ) with respect to parameters is summarized with the following algorithm.

Algorithm 3.4. *(Computation of derivatives with respect to parameters) Let* $(K, W, \lambda)_\varepsilon$ *be implicit functions of* ε *by equations* (12) *and* (16). *Find* $\partial_\varepsilon K$, $\partial_\varepsilon W$, *and* $\partial_\varepsilon \lambda$ *by following these steps:*

(1) *Compute* $P(\theta,\varphi)$ *and* $S^1(\theta,\varphi)$ *by following Algorithm 3.1.*
(2) *Compute* $\eta(\theta,\varphi)$, *the right-hand side of the cohomological equations given in* (61), *from* (62).
(3) *Solve* (51) *and* (53) *as non-small divisors cohomological equations in order to obtain* $\xi^2(\theta,\varphi)$ *and* $\xi^4(\theta,\varphi)$.
(4) *Solve* (52) *as small divisors cohomological equations in order to obtain its zero-average solution* $\tilde\xi^3(\theta,\varphi)$.
(5) *Compute* $\langle S^1\rangle$, *and the right-hand side of the linear system,* (54) *and solve it in order to obtain* ξ^3_0.
(6) *Solve* (50) *as small divisors cohomological equations in order to obtain* $\xi^1(\theta,\varphi)$ *with* $\langle\xi^1\rangle = 0$.
(7) *Set* $\partial_\varepsilon K(\theta,\varphi) \leftarrow P(\theta,\varphi)\xi(\theta,\varphi)$.
(8) *Compute* $E^{\partial_\varepsilon W}(\theta,\varphi)$ *from* (64).

(9) *Compute* $\eta(\theta,\varphi)$*, the right-hand side of the cohomological equations given in* (65)*, from* (66)*.*
(10) *Solve* (59)*,* (60)*, and* (57) *as non-small divisors cohomological equations in order to obtain* $\xi^3(\theta,\varphi)$*,* $\xi^4(\theta,\varphi)$*, and* $\xi^1(\theta,\varphi)$*, respectively.*
(11) *Take* $\partial_\varepsilon\lambda = -\langle\eta^2\rangle$*.*
(12) *Solve*

$$\lambda\xi^2(\theta,\varphi) - \lambda\xi^2(\theta,\varphi) - \partial_\varepsilon\lambda = \eta^2(\theta,\varphi)$$

as a small divisors cohomological equation with $\langle\xi^2\rangle = 0$
(13) *Set* $\partial_\varepsilon W(\theta,\varphi) \leftarrow P(\theta,\varphi)\xi(\theta,\varphi)$*.*

3.4. **Comments on implementations.** For every function $\zeta : \mathbb{T}^{d-1}\times\mathbb{T}^\ell \to \mathbb{R}$, we use its Fourier representation and their grid representation. The Fourier representation is given in terms of Fourier coefficients $\{\hat{\zeta}_{kj}\} \in \mathbb{C}$, with $k \in \mathbb{Z}^{d-1}$ and $j \in \mathbb{Z}^\ell$, and the grid representation is given by the values $\{\zeta_{kj}\}$ of ζ in an equally spaced grid of $\mathbb{T}^{d-1}\times\mathbb{T}^\ell$. We can switch between both representations with the linear one-to-one map provided by the Discrete Fourier Transform (DFT). Operations such as phase shifts, differentiation, or solving cohomological equations can be done efficiently in Fourier space whereas numerical integration or evaluation of vector fields can be done more efficiently in the grid representation. We switch between both representations according to the operations to be performed. See e.g. [HM21] for details.

In practice, we can only work with truncated series. Furthermore, the DFT only provides approximate coefficients, that cannot in general be directly identified with the Fourier coefficients. Instead, for each coefficient $\hat{\zeta}_{kj}$, we use the DFT coefficient that best approximates it, see e.g. [Hen79] for details.

The unstable Floquet multiplier of $\mathcal{K}$ can be large, which would compromise the convergence of the method. In the numerical explorations of Section 4, instead of solving Eqs. (12) and (16), we follow a multiple shooting approach. We consider multiple tori $\{\mathcal{K}_i\}_{i=0}^{m-1}$ and bundles $\{\mathcal{W}_i\}_{i=0}^{m-1}$ parameterized by $\{K_i\}_{i=0}^{m-1}$ and $\{W_i\}_{i=0}^{m-1}$ with $K_i : \mathbb{T}^{d-1}\times\mathbb{T}^\ell \to U$ and $W_i : \mathbb{T}^{d-1}\times\mathbb{T}^\ell \to \mathbb{R}^{2n}$ such that

$$\phi_{T/m}\big(K_i(\theta,\varphi),\varphi\big) - K_{i+1}(\bar\theta_m,\bar\varphi_m) = 0, \tag{67}$$

$$\mathrm{D}_z\phi_{T/m}\big(K_i(\theta,\varphi),\varphi\big)W_i(\theta,\varphi) - \lambda^{\frac{1}{m}}W_{i+1}(\bar\theta_m,\bar\varphi_m) = 0 \tag{68}$$

for $i = 1,...,m-1$, where $\bar\theta_m := \theta + \omega/m$ and $\bar\varphi_m := \varphi + \alpha/m$. The subindex in K and W is defined modulo m. We choose m such that $|\lambda|^{\frac{1}{m}}$ is small enough. The methodology described in Section 3 generalizes with some extra work for Eqs. (67) and (68). For the sake of clarity, we have described the method for $m = 1$. Nonetheless, the generalization from $m = 1$ to $m > 1$ is analogous to the generalization in the autonomous case which can be found in [HM21].

The evaluation of flow maps and the variational equations require numerical integration that can be costly for high-dimensional tori. Nonetheless, numerical integration is easily parallelizable by assigning trajectories to different threads.

To prevent numerical instabilities, we implement a lowpass filter after each Newton step on K and W for the approximate Fourier coefficients of the parameterizations, i.e., at the end of Algorithms 3.2 and 3.3. For simplicity, assume $\mathcal{K}$ is a 2-dimensional torus with a grid of size $N_1 \times N_2$—which is the test case of Section 4. The filtering strategy consists of setting to zero the coefficients for $|k| > k_f$ and $|j| > j_f$ for the values $k_f = r_f \cdot N_1$ and $j_f = r_f \cdot N_2$, where $r_f \in \left[\frac{1}{4}, \frac{1}{2}\right)$ is some filtering factor. Because of this filtering strategy, the effective number of approximate Fourier coefficients is not $N_1 \times N_2$.

Since we are working with truncated Fourier series, we need to decide on the number of Fourier coefficients. This number needs to be large enough so the series allow the parameterizations to meet their required error tolerance in the invariance equations. The necessary number of coefficients might change throughout the continuations so we also need a strategy to adjust the grid sizes of the invariant objects. Since our objects are real analytic, their Fourier coefficients decay exponentially fast. Our strategy is based on controlling this decay. In order to do so, we compute the tails of the truncated series. For functions $\zeta : \mathbb{T} \times \mathbb{T} \to \mathbb{R}$, we compute the tails in the internal phase θ and the external phase φ as

$$t_\theta(\zeta) = \sum_{|k|>k_t, |j|<j_t} |\hat{\zeta}_{kj}|, \qquad t_\varphi(\zeta) = \sum_{|k|<k_t, |j|>j_t} |\hat{\zeta}_{kj}|,$$

for $k_t = r_t \cdot N_1$, $j_t = r_t \cdot N_2$, where r_t is some tail factor such that $r_t < r_f$. For the case where $\zeta : \mathbb{T} \times \mathbb{T} \to \mathbb{R}^{2n}$, we consider t_θ and t_φ to act component-wise.

Furthermore, throughout the continuations on ε, the necessary step size of the continuation procedure needs to be adjusted. We conclude this section with a proposal in Algorithm 3.5 for the continuation of generating tori, bundles, and Floquet multipliers that is an adaptation for our case of Algorithm 3.6.1 in [HM21]. The main difference is that in the algorithm of [HM21], a strategy to reduce the number of Fourier coefficients in the parameterizations is necessary whereas in Algorithm 3.5, we require a strategy to control the decay of the coefficients in the different phases of K and W to adjust the grid sizes of the parameterizations.

Let us represent the parameterizations of the invariant objects and the Floquet multiplier for some parameter ε as $\mathcal{T}_\varepsilon = (\varepsilon, K, W, \lambda)$, for which we consider the norm

$$\|\mathcal{T}_\varepsilon\| := \left(\varepsilon^2 + \lambda^2 + \langle \|K\|_2^2 \rangle + \langle \|W\|_2^2 \rangle\right)^{\frac{1}{2}},$$

where $\|K\|_2$ stands for the map $(\theta,\varphi)\mapsto \|K(\theta,\varphi)\|_2$, $\|\cdot\|_2$ denotes the Euclidean norm in $\mathbb{R}^{2n}$, and $\|W\|_2$ is the analogous map.

Let us estimate the error in the torus and bundle as follows

$$\begin{aligned}\mathrm{err}^K(\mathcal{T}_\varepsilon) &= \max_{\substack{0\le k<N_1\\0\le j<N_2}} \|E^K(k/N_1, j/N_2)\|_\infty,\\ \mathrm{err}^W(\mathcal{T}_\varepsilon) &= \max_{\substack{0\le k<N_1\\0\le j<N_2}} \|E^W(k/N_1, j/N_2)\|_\infty,\end{aligned}$$

where $\|\cdot\|_\infty$ stands for the supremum norm in $\mathbb{R}^{2n}$. Then, a proposal for the continuation of tori and their bundles is summarized in the following algorithm.

Algorithm 3.5. *(Continuation implementation) Let $\mathcal{T}_\varepsilon$ be an approximately invariant torus, bundle, and Floquet multiplier for some value of the external parameter ε and some values of the flying time T and rotation vectors ω and α. Let K and W have grid representations of size $N_1\times N_2$, let $\epsilon_K,\epsilon_W,\epsilon_t$ be tolerances, r_t some tail factor, and $n_{max}, n_\varepsilon, n_{des}, n_t$ be integers. Assume we have a suggested continuation step $\Delta\varepsilon$. Compute a new torus, bundle, and Floquet multiplier $\mathcal{T}_{\varepsilon'}$ for a new value of the external parameter ε' and fixed T, ω, and α as follows:*

(1) *Compute $\partial_\varepsilon K, \partial_\varepsilon W$, and $\partial_\varepsilon\lambda$ following algorithm 3.4 and set the continuation direction $\delta \leftarrow (1,\partial_\varepsilon K,\partial_\varepsilon W,\partial_\varepsilon\lambda)$.*
(2) *Set $\Delta\mathcal{T}_\varepsilon \leftarrow \delta/\|\delta\|$ and $\mathcal{T}_{\varepsilon'} \leftarrow \mathcal{T}_\varepsilon + \Delta\varepsilon\Delta\mathcal{T}_\varepsilon$.*
(3) *Perform Newton steps on $\mathcal{T}_{\varepsilon'}$ by following algorithms 3.2 and 3.3 until $\mathrm{err}^K(\mathcal{T}_{\varepsilon'}) < \epsilon_K$ and $\mathrm{err}^W(\mathcal{T}_{\varepsilon'}) < \epsilon_W$ or up to n_{max} times.*
(4) *If $\mathrm{err}^K(\mathcal{T}_{\varepsilon'}) < \epsilon_K$ and $\mathrm{err}^W(\mathcal{T}_{\varepsilon'}) < \epsilon_W$, let n_{it} be the number of Newton iterations and go to step 8.*
(5) *Go to step 2 with $\Delta\varepsilon \leftarrow \frac{1}{2}\Delta\varepsilon$ up to n_ε times.*
(6) *Compute $\|t_\theta(K)\|_\infty$ and $\|t_\varphi(K)\|_\infty$.*
(7) *If $\|t_\theta(K)\|_\infty > \epsilon_t$ and $\|t_\varphi(K)\|_\infty > \epsilon_t$, set $N_1 \leftarrow 2N_1$ and $N_2 \leftarrow 2N_2$. Otherwise, set $N_1 \leftarrow 2N_1$ if $\|t_\theta(K)\|_\infty > \|t_\varphi(K)\|_\infty$ and $N_2 \leftarrow 2N_2$ if $\|t_\varphi(K)\|_\infty > \|t_\theta(K)\|_\infty$. Go to step 1; try up to n_t times.*
(8) *Set $\mathcal{T}_\varepsilon \leftarrow \mathcal{T}_{\varepsilon'}, \Delta\varepsilon \leftarrow \frac{n_{des}}{n_{it}}\Delta\varepsilon$ and go to step 1.*

4. An application: the elliptic restricted three body problem

In this section, we apply our method to the periodic Hamiltonian system given by the Elliptic Restricted Three Body Problem (ERTBP). The strategy we follow consists of taking families of 2D partially hyperbolic invariant tori in the Circular Restricted Three Body Problem (CRTBP) and lift them to the elliptic problem as 3D partially hyperbolic invariant tori through continuation in the eccentricity as described in Section 3. In practice, we compute parameterizations of 2D generating tori together with their stable, unstable, and center generating bundles.

For the numerical explorations, we have used a Fujitsu Siemens CELSIUS R930N workstation with two 12-core Intel Xeon E5-2630v2 at 2.60GHz running Debian GNU/Linux 11. The algorithms were written in C, compiled with GCC 10.2.1 and linked against Glibc 2.31, LAPACK 3.9.0, and FFTW 3.3.8. The numerical integration was parallelized using OpenMP 4.5.

4.1. **Dynamics.** The ERTBP models the motion of a small body of negligible mass in the gravitational vector field generated by two other massive bodies, known as primaries, moving in elliptical orbits according to two-body dynamics.

Let us denote by m_1 and m_2 the masses of the primary bodies and let us also define the parameter $\mu := \frac{m_2}{m_1+m_2}$. It is possible to define a rotating and pulsating frame after a suitable rescaling in space and time where the primaries of mass m_1 and m_2 are at $(\mu, 0, 0)$ and $(\mu - 1, 0, 0)$, respectively, and their period of revolution is 2π, see [Sze67] for details. The dynamics for the third body are then given by the periodic Hamiltonian

$$\begin{aligned} H(x,p,\varphi) &= \frac{1}{2}[(p_1+x_2)^2+(p_2-x_1)^2+p_3^2+x_3^2] \\ &\quad - \frac{1}{1+e\cos f}\left[\frac{1}{2}(x_1^2+x_2^2+x_3^2)+\frac{1-\mu}{r_1}+\frac{\mu}{r_2}\right], \end{aligned}$$

with $x \in \mathbb{R}^3$ positions, $p \in \mathbb{R}^3$ momenta, $r_1^2 = (x_1-\mu)^2+x_2^2+x_3^2, r_2^2 = (x_1+1-\mu)^2+x_2^2+x_3^2$, and $e \in \mathbb{R}$ the eccentricity of the elliptic orbit of the primaries. The true anomaly $f := 2\pi\varphi$, with $\varphi \in \mathbb{T}$, is the angle that parameterizes the orbit of the primaries and moves according to the frequency $\dot{\varphi} = \hat{\alpha} = 1/2\pi$.

The ERTBP has five fixed points, known as the Lagrange points, denoted by L_i with $i = 1, 2, ..., 5$. The coordinates of these equilibrium points coincide with the coordinates of the fixed points in the circular problem. The collinear solutions L_1, L_2, and L_3 are unstable for any combination of μ and e whereas the stability of the triangular points, L_4 and L_5, depends on these two parameters. For their values in the Sun-Earth system, that is $\mu = 3.040357143 \cdot 10^{-6}$ and $e = 0.01671123$, the triangular Lagrange points are linearly stable (see e.g. [Sze67] for details).

The persistence of the fixed points in the elliptic problem does not generalize to other invariant objects. Periodic solutions only exist in resonance with the frequency of the primaries. Furthermore, the frequency of the primaries, i.e. the external frequency $\hat{\alpha}$, is added to invariant objects such as periodic orbits and invariant tori of the CRTBP increasing the dimension by one of their counterparts in the elliptic case. That way, (non-resonant) periodic orbits survive as 2D tori while the classical Lissajous and quasi-halo orbits become 3D tori—this will be our case study.

4.2. **From the CRTBP to the ERTBP.** As we mentioned previously, we will lift invariant tori and bundles from the CRTBP to the ERTBP. In this section, we include some details on the families of tori that we computed in the circular problem: tori in the center manifold of the L_1 point.

The L_1 point in the CRTBP is of type center×center×saddle; that is

$$\mathrm{Spec}\mathrm{D}X_H(L_1) = \{\boldsymbol{i}2\pi\hat{\omega}_p^0, -\boldsymbol{i}2\pi\hat{\omega}_p^0, \boldsymbol{i}2\pi\hat{\omega}_v^0, -\boldsymbol{i}2\pi\hat{\omega}_v^0, \lambda^0, -\lambda^0\},$$

with a value of the Hamiltonian h^0. Thus, there is a 4-dimensional center manifold generated by the central part of L_1 that contains invariant objects.

The Lyapunov center theorem (see e.g. [MHO09, SM95]) ensures that there exists two 2-dimensional manifolds inside the center manifold filled with families of periodic orbits: the planar and the vertical Lyapunov families. These families present bifurcations that give birth to new families such as the halo family and other more exotic orbits (see e.g. [DDP03]). We can parameterize the orbits in these families in a large neighborhood of the L_1 point by their value of the Hamiltonian.

Besides the 2-dimensional manifolds of periodic orbits, the center manifold is also filled with 2-dimensional tori that exist around periodic orbits with a central part. Let us focus on the tori around vertical Lyapunov orbits. Let $\hat{\omega}_p$ and $\hat{\omega}_v$ be the frequencies of any torus such that $\hat{\omega}_p \to \hat{\omega}_p^0$ and $\hat{\omega}_v \to \hat{\omega}_v^0$ when $h \to h^0$, see Remark 2.2 on the non-uniqueness of the frequencies. Following [HM21], we define the rotation number as $\rho := \hat{\omega}_p/\hat{\omega}_v - 1$. We can then use the Hamiltonian h and ρ to represent the family of 2-dimensional tori around the vertical Lyapunov orbits. These two parameters uniquely determine each torus. Analogous representations can be obtained for the tori around planar Lyapunov and halo orbits, see [GM01, HM21] for a full description.

For $\mu = 3.040357143 \cdot 10^{-6}$ and $e = 0$, we selected 77 equally spaced values of ρ between 0.03565 and 0.0961 for the Sun-Earth system and "nobilized"[1] them with an absolute tolerance of 1.6×10^{-4}. Then, we performed continuations in the flying time T for each value of $\omega = \rho$, following the methodology from [HM21], and obtained the family of tori around vertical Lyapunov orbits in the CRTBP. The results are gathered in Fig. 2 where we plot the rotation number and the Hamiltonian as well as the grid size of the parameterizations in the color map for each of the 8971 tori computed.

[1]A noble number is one whose continued fraction expansion coefficients are equal to one from a position onward.

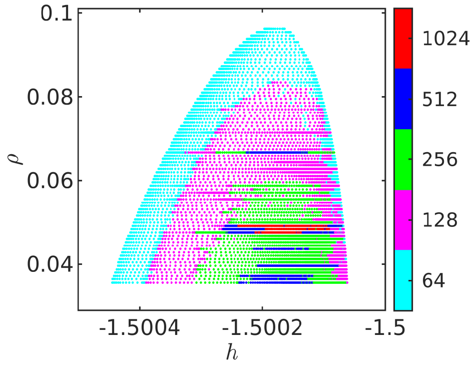

FIGURE 2. Energy-rotation number representation in the CRTBP for the Lissajous family around L_1 vertical orbits for the Sun-Earth mass parameter. The color map represents the grid size of the parameterizations.

4.3. **Numerical explorations in the ERTBP.** In this case study, the generating tori $\mathcal{K}$ are 2-dimensional and the generated tori $\hat{\mathcal{K}}$ are 3-dimensional. To initialize the algorithms, we use the autonomous tori from the CRTBP with a grid size in the internal phase as given in Fig. 2. For the initial grid size in the external phase, we took $N_2 = 16$. Since the generating tori in the CRTBP are 1-dimensional, we obtain the 2-dimensional generators by setting the approximate Fourier coefficients $\hat{\xi}_{kj}$ to zero for $|j| > 0$. Equivalently, we can construct the generators as in (14). In algorithm 3.5, we use $\epsilon^K = 10^{-9}, \epsilon^W = 10^{-5}, \epsilon^t = 10^{-9}, r_t = 1/5, n_{max} = 6, n_\varepsilon = 3, n_{des} = 4$, and $n_t = 2$. We set a maximum of 1024 Fourier coefficients in each phase and for the multiple shooting approach, we take $m = 4$. We set the continuations to reach the eccentricity of the Sun-Earth system; that is, $e = 0.01671123$. It is worth mentioning that we set $\epsilon^K = 10^{-9}$ for such an exhaustive numerical exploration, but we manage to get errors in the invariance equations of the order of 10^{-15} for some tori.

The results of our numerical explorations are gathered in Fig. 3. Out of the 8971 tori computed in the CRTBP, 4457 reached the Sun-Earth eccentricity. Each torus in the Figure is labeled by its value of the internal rotation number and the value of the Hamiltonian of the torus in the CRTBP used to initiate the continuations. Note that we use h simply as a label with no dynamical implications. In the color map of Fig. 3, we represent the grid size in the internal phase θ (left) and the external phase φ (right) only of the tori that reached the eccentricity of the Sun-Earth system.

We can observe that not all continuations reach the required value of the eccentricity. Certain empty "lines", where the continuations fail, are present, which suggests the existence of a dynamical barrier. It turns out that these lines correspond to resonances between the

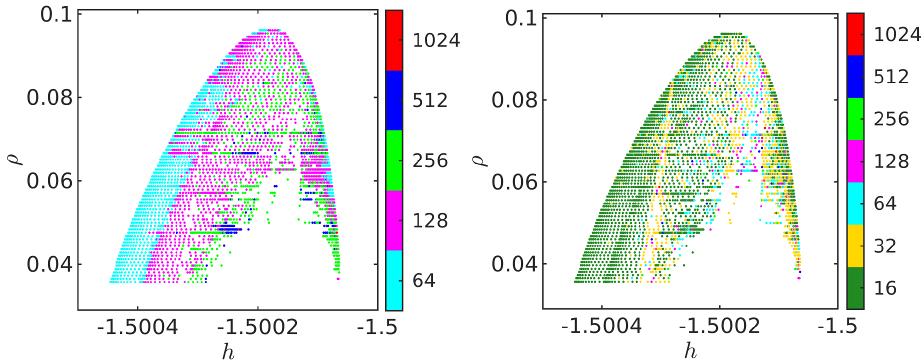

FIGURE 3. Energy-rotation number representation in the ERTBP for the Lissajous family around L_1 vertical orbits for the Sun-Earth mass parameter. The color map represents the grid size of the internal phase (left) and the external phase (right).

frequencies of the 3-dimensional tori, see Section 4.4. For values of $\rho < 0.06$, there is also a gap in the energy-rotation number representation. The lack of convergence in this region is related to resonances and also to the existence of homoclinic and heteroclinic tangles. We will come back to this issue in Section 4.5.

From the numerical explorations we can see that, generally, tori in the ERTBP do not need a large number of approximate Fourier coefficients in the external phase, see Fig. 3 (right), which suggests that our tori are more analytic in the phase φ. Note that φ is essentially time and tori tend to be more analytic in the temporal direction, which is in agreement with our results.

Close to resonances, the number of coefficients needed increases. We also observe an increase in the number of coefficients for the tori surrounding the region where homoclinic and heteroclinic tangles are present. Resonances and homoclinic and heteroclinic tangles are responsible for the breakdown of tori, see [Chi79, dlLO06, OS87]. The fact that more coefficients are necessary for the parameterizations close to such cases reveals that the tori are losing regularity because they are breaking down.

In order to lift the autonomous tori to the elliptic problem, we see that it does not suffice to simply add coefficients in the external phase. When we compare Fig. 2 and Fig. 3 (left), the number of coefficients in the internal phase changes. Throughout the continuations, it was seen that for a given torus, sometimes it was necessary to increase the number of coefficients in the phase θ and sometimes in the phase φ. It is therefore key to control the decay of the Fourier coefficients as it has been described in Section 3.4.

Lastly, we include in Fig. 4.3 some plots in the configuration space of 3-dimensional tori (red) and their 2-dimensional generators (black) for a family with $\rho = 0.071461$. They can be seen as “fattened” with respect to their CRTBP. Such “fattening” is clearly seen in the results from Section 4.5.

The behavior of the family of tori for fixed ρ is qualitatively very similar to their autonomous counterparts in the CRTBP, see [HM21]. The family begins with a torus close to a vertical Lyapunov orbit and, with increasing energy, the tori increase in size and start to bend. Then, tori approach a vertical Lyapunov orbit of higher energy where the family collapses.

Remark 4.1. *To obtain the results presented in Fig. 3, we did several runs of Algorithm 3.5 for different values of the filtering factor for the lowpass filter described in Section 3.4. To give an idea of the computing time, for the family* $\rho = 0.089837$, *we performed continuations in e of 30 tori from the CRTBP to the Sun–Earth ERTBP in* 4725.57 *seconds. This is the total computing time, the wall-clock time is roughly the total computing time divided by the number of threads; 24 in our case, so each of the previous continuations was done in roughly 6.6 seconds. Note that not all tori take the same time to compute. Computations close to resonances or close to homoclinic connections can take significantly longer.*

4.4. **Resonances.** The vector of frequencies $(\hat{\omega}, \hat{\alpha})$ was assumed to be sufficiently non-resonant; that is, Diophantine. When this assumption does not hold, there is a dynamical obstruction to the existence of invariant tori.

Let $\kappa = (\kappa_1, \kappa_2, \kappa_3)$ be a 3-tuple. The vectors of frequencies $\hat{\omega} = (\frac{\rho}{T}, \frac{1}{T})$ and $\hat{\alpha} = \frac{1}{2\pi}$ are in p-order resonance when $|\kappa|_1 = p$ and

$$\mathcal{R}_\kappa := \kappa_1 \frac{\rho}{T} + \kappa_2 \frac{1}{T} + \kappa_3 \frac{1}{2\pi}, \tag{69}$$

becomes zero. The final tori obtained in the Sun-Earth ERTBP, represented in Fig. 3, are grouped in constant-ρ families but, througout each constant-ρ family, the flying time T varies. For certain κ and ρ, $\mathcal{R}_k$ might become small, revealing that the frequencies of the generated tori whithin the constant-ρ family are approaching resonances. Note that for given κ, with $|\kappa|_1 = p$, $\mathcal{R}_k = 0$ defines p-resonant lines. To visualize these resonances in the energy-rotation number representation, we first examine the tori computed in the CRTBP. We look for 3-tuples $\bar{\kappa}$ such that $\mathcal{R}_{\bar{\kappa}} < \epsilon^{\mathcal{R}}$ up to a maximum order $\bar{p}$. We took $\epsilon^{\mathcal{R}} = 10^{-4}$ and $\bar{p} = 10$. Once we obtain the 3-tuples $\bar{\kappa}$, we compute the lines $\mathcal{R}_{\bar{\kappa}} = 0$ and obtain $\rho_{\bar{\kappa}} = \rho_{\bar{\kappa}}(T)$. Then, we use the values of h, ρ, and T of the grid of tori computed in the CRTBP to obtain through inverse cubic interpolation, for each line $\mathcal{R}_{\bar{\kappa}} = 0$, the curve $\rho_{\bar{\kappa}} = \rho_{\bar{\kappa}} \circ T(h)$. The results are shown in Fig. 5.

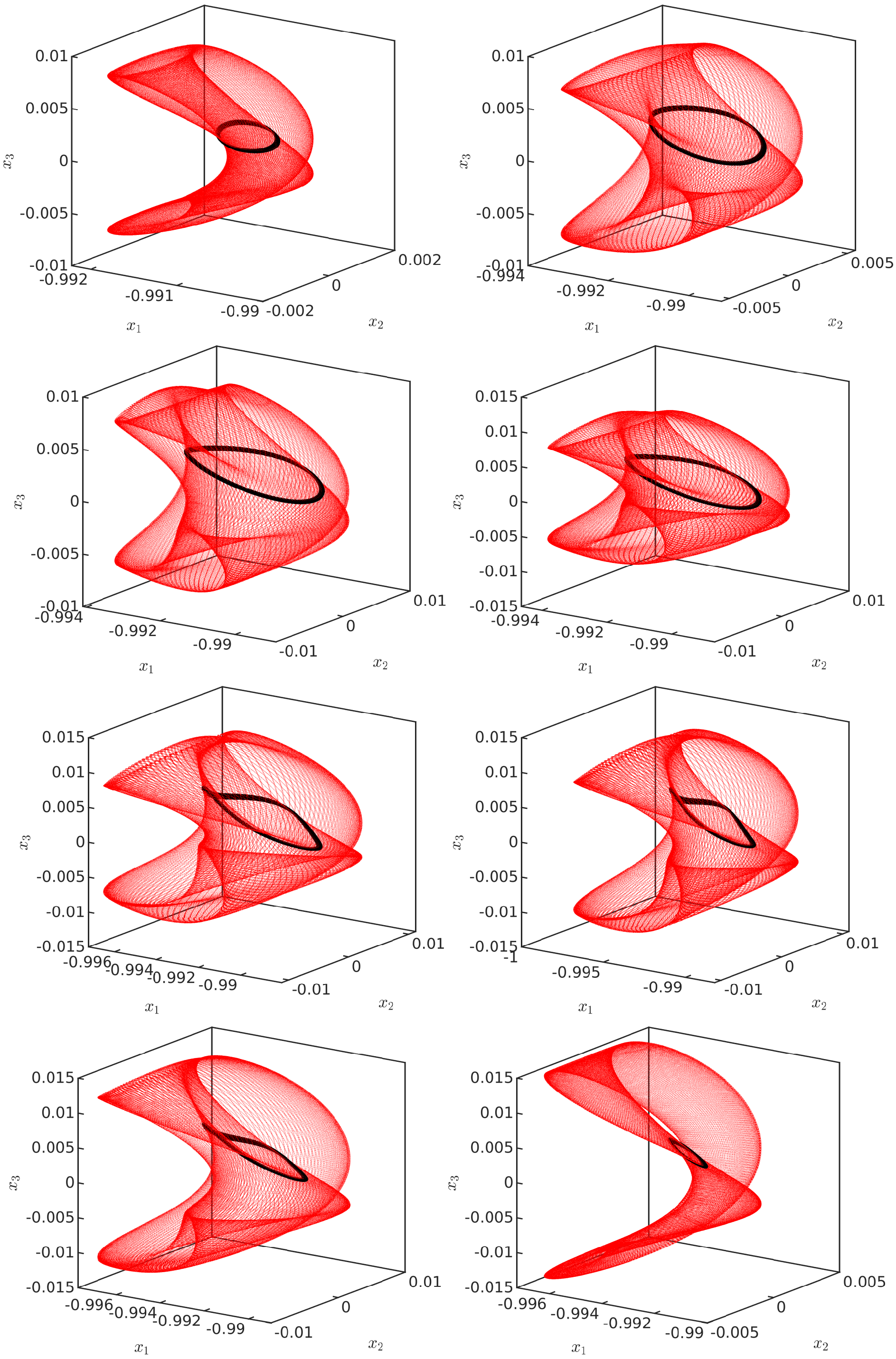

FIGURE 4. Projection onto the configuration space of 3-dimensional generated tori (red) and 2-dimensional generating tori (black) for the family $\rho = 0.071461$. From left to right $h = -1.50033, -1.50030, -1.50028, -1.50026, -1.50017, -1.50014, -1.50012, -1.50010$.

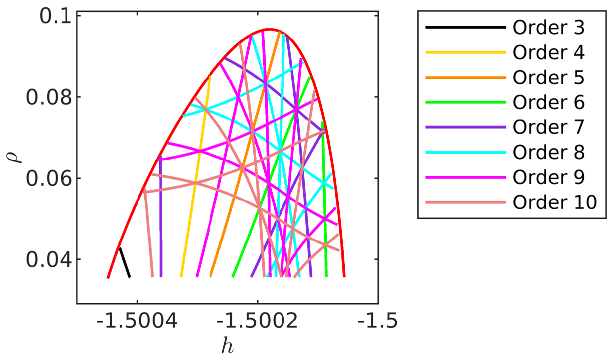

FIGURE 5. Resonant curves up to order 10 for the tori in the ERTBP for the Sun-Earth mass parameters.

It is clear that when lifting the tori from the CRTBP to the ERTBP, the frequencies can become resonant for a large subset of the autonomous tori. We observe that for $h \geq -1.5002$, there is an accumulation of resonant curves in the energy-rotation number representation which explains the gap where few tori converged. The accumulation of resonant curves also explains why, when comparing Fig. 2 and Fig 3 (left), more coefficients are necessary for the parameterizations of the tori that reached the Sun-Earth eccentricity.

Note the correspondence between the resonant curves and the results from Fig. 3—the absence of tori in the region surrounded by tori with $N_2 = 32$ in Fig. 3 (right) corresponds to an order 4 resonance. Other resonant curves can be appreciated but are more subtle—the lower the order of the resonance, the bigger the obstruction to convergence. Due to the presence of resonances, performing continuations for each torus in the CRTBP is a more robust approach than performing them in the ERTBP. When the method tries to compute a resonant torus, it will simply fail and move to the next, whereas if continuations where done in the ERTBP, the method would have to jump through all the resonances it encounters.

4.5. **Poincaré representation.** As we pointed out, the Hamiltonian in the ERTBP is not constant. Therefore, we cannot obtain the isoenergetic sections of the center manifold commonly seen in studies for the CRTBP, see e.g. [JM99, GM01, GJSM01]. Nonetheless, in this section we show some analogous results. In addition to the numerical results already presented, we have also taken tori in the CRTBP around vertical and halo orbits within a level set of the Hamiltonian, lifted them to the Sun-Earth ERTBP, and computed a Poincaré section with $\Sigma = \{x, p \in \mathbb{R}^3 |\ x_3 = 0, p_3 > 0\}$.

We explore the level set $H = -1.5002$, value that crosses the region with the large gap, see Fig. 3. The results are gathered in Fig. 6. On the left, we show (in red) the intersections of the tori of the CRTBP that, when used as seeds of continuations in the eccentricity e, reach the Sun-Earth ERTBP. The sections of the 3-dimensional tori at the end of each of the previous continuations are shown in Fig. 6 right. In order to have some reference of where the families of tori end, we show in black the intersections of the last tori computed in the CRTBP around vertical and halo orbits.

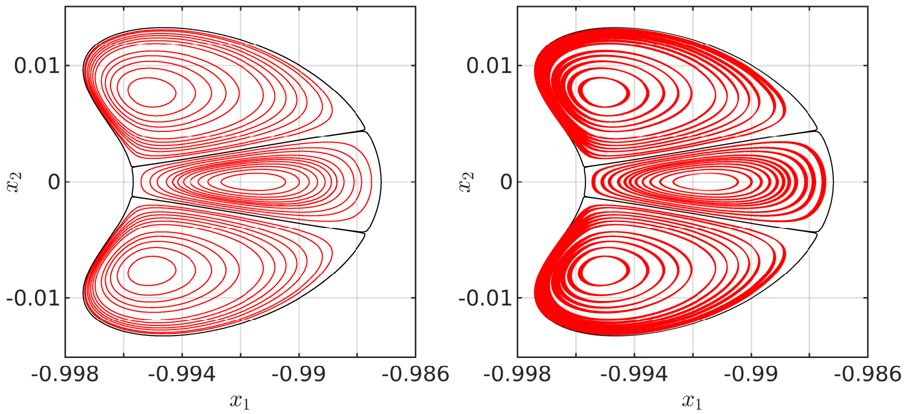

FIGURE 6. Intersections in red of Lissajous and quasi-halo tori with Σ in the CRTBP (left) and in the ERTBP (right). In black, we show the intersections of the last tori computed for each family in the CRTBP. The tori were computed from the level set $H = -1.5002$ in the CRTBP.

We first observe that since the tori in the ERTBP are 3-dimensional, the intersections with Σ are 2-dimensional. This allows us to somewhat see the "fattening" of each torus due to the time dependency of the Hamiltonian. This fattening has important implications for the convergence of our method in the region of the energy-rotation number where tori approach homoclinic and heteroclinic connections.

In the CRTBP, there is a range of the Hamiltonian where there exist tori that approach double homoclinic connections of planar Lyapunov orbits. For larger energy values, there exist heteroclinic connections between the so called "axial" orbits. These connections act as separatrices between the Lissajous and quasi-halo families. An example of a torus approaching such connections is shown in Fig. 8 of [HM21], where a torus around a vertical orbit approaches two vertically symmetric quasi-halo tori. The existence of transverse homoclinic and heteroclinic points is one known mechanism for breakdown of invariant tori, see [Chi79, dlLO06, OS87], and the tori in the CRTBP that approach connections were found for small values of ρ, see [HM21].

Non-resonant periodic orbits in the CRTBP survive as 2-dimensional tori in the ERTBP, so there might be even more connections than in the CRTBP. Together with the fact that tori in the ERTBP have been "fattened", suggests that there might be a larger set of tori in the ERTBP that are sufficiently close to homoclinic and heteroclinic connections for the method to fail.

Lastly, in Fig. 7, we show in the configuration space plots of the Lissajous (red) and quasi-halo (blue) tori whose intersections with Σ are largest in the Poincaré section of Fig. 6. That is, the largest Lissajous and quasi-halo tori that reached the Sun-Earth ERTBP from the level set $H = -1.5002$ in the Sun-Earth CRTBP. For easier visualization, of the two symmetric quasi-halo tori of the energy level only one is shown. We can observe the proximity between the tori in the configuration space (similar plots can be obtained with other projections) and how they almost merge.

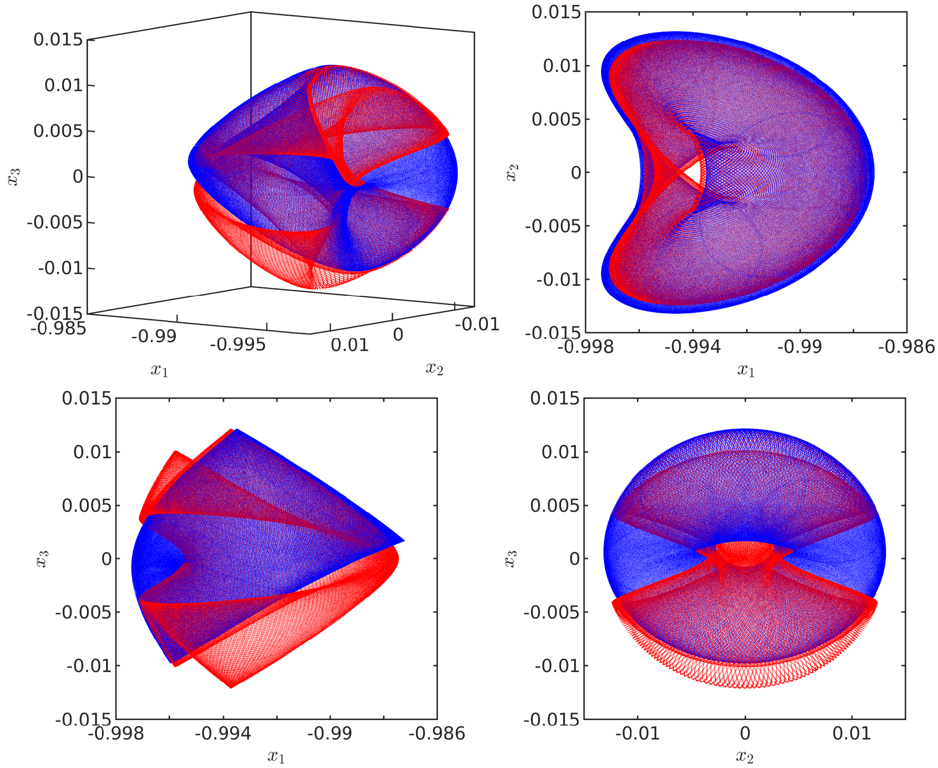

FIGURE 7. Largest Lissajous (red) and quasi-halo (blue) tori, and their projections, computed in the Sun-Earth ERTBP from the level set $H = -1.5002$ in the CRTBP

5. Conclusions

In this work, we presented a general and efficient method to compute parameterizations of invariant tori and their bundles in quasi-periodic Hamiltonian systems with an arbitrary number of frequencies. To this end, we generalized flow map parameterization methods applicable in autonomous settings. This generalization required the development of the notions of fiberwise isotropy of invariant tori and fiberwise Lagrangian subspaces. We obtained primitive functions of quasi-periodic time-t maps and, in a more general framework, we introduced the concepts of fiberwise symplectic deformations and moment maps. All of these notions are vital for our constructions and for eventual proofs, using KAM techniques, of the existence of invariant objects and their regularity with respect to parameters.

We manage to reduce the dimension of the phase space by considering appropriate functional equations. We also reduce the dimension of our objects by using flow maps. Instead of using periods associated to the Hamiltonian we use periods associated to the internal frequencies of tori—which allow us to directly compute invariant tori in quasi-periodic Hamiltonian systems from tori in autonomous systems in an efficient and general setting. We also provided a continuation method, under the parameterization method paradigm, for continuation of invariant tori and bundles with respect to parameters of the Hamiltonian.

We tested our method in a periodic Hamiltonian system: the Elliptic Restricted Three Body Problem (ERTBP). We computed a large grid of 3-dimensional invariant tori and their invariant bundles, gaining qualitative insight into the behavior of the ERTBP. From the numerical explorations, we observed that tori and bundles are more regular in the external phase. This implies that less coefficients are required for their computation. Consequently, it is advantageous to include external phases in the parameterizations. Additionally, we observed that for a large set of tori the frequencies can be in resonance; which is an obstruction to their existence. Therefore, computing tori by lifting them from an autonomous system is a more robust approach than performing continuations directly in the ERTBP.

Acknowledgements

This work has been supported by the Spanish grants MCINN-AEI PID2020-118281GB-C31 and PID2021-125535NB-I00, the Catalan grant 2021 SGR 00113, the Severo Ochoa and María de Maeztu Program for Centers and Units of Excellence in R&D (CEX2020-001084-M) of the Spanish Research Agency, the European Union's Horizon 2020 research and innovation program under the Marie Skłodowska-Curie grant agreement No 734557, the Secretariat for Universities and Research of the Ministry of Business and Knowledge of the Government of Catalonia, and by the European Social Fund.

We would like to thank Àngel Jorba and Arturo Vieiro for providing and maintaining some workstations at UB on which an important part of the computations has been done. We would also like to acknowledge the work of the free software community in providing all the software tools we have used.

Appendix A. Quadratically small averages

For the Newton step described in Section 3.2.1 to be consistent, we need the averages of η^3 given by

$$\eta^3(\theta,\varphi) = \begin{pmatrix} \mathrm{D}_\theta K(\bar\theta,\bar\varphi)^\top \Omega\big(K(\bar\theta,\bar\varphi)\big) E^K(\theta,\varphi) \\ \mathcal{X}_H(\bar\theta,\bar\varphi)^\top \Omega\big(K(\bar\theta,\bar\varphi)\big) E^K(\theta,\varphi) \end{pmatrix} =: \begin{pmatrix} \eta^{31}(\theta,\varphi) \\ \eta^{32}(\theta,\varphi) \end{pmatrix}$$

to be quadratically small with respect to the error in the torus invariance E^K. Note that for some suitable norm, the derivatives of E^K can be controlled by $\|E^K\|$ using Cauchy estimates. The following lemma provides the explicit formulas for $\langle \eta^3 \rangle$.

Lemma A.1. *The averages of η^{31} and η^{32} are given by*

$$\langle \eta^{31} \rangle = \left\langle \mathrm{D}_\theta E^K(\theta,\varphi)^\top \Delta^1 a(\theta,\varphi) + \mathrm{D}_\theta K(\bar\theta,\bar\varphi)^\top \Delta^2 a(\theta,\varphi) \right\rangle$$
$$\langle \eta^{32} \rangle = \left\langle \Delta^2 H(\theta,\varphi) \right\rangle - \left\langle \Delta^1 a(\theta,\varphi)^\top \mathrm{D}_\varphi E^K(\theta,\varphi)\hat\alpha \right\rangle - \left\langle \Delta^2 a(\theta,\varphi)^\top \mathrm{D}_\varphi K(\bar\theta,\bar\varphi)\hat\alpha \right\rangle,$$

where the Taylor remainders Δ^i of order i in E^K are given by

$$\begin{aligned}
\Delta^1 a(\theta,\varphi) &:= a\big(\phi_T(K(\theta,\varphi),\varphi)\big) - a\big(K(\bar\theta,\bar\varphi)\big) \\
&= \int_0^1 \mathrm{D}a\big(K(\bar\theta,\bar\varphi) + sE^K(\theta,\varphi)\big)E^K(\theta,\varphi)\, ds, \\
\Delta^2 a(\theta,\varphi) &:= a\big(\phi_T(K(\theta,\varphi),\varphi)\big) - a\big(K(\bar\theta,\bar\varphi)\big) - \mathrm{D}a\big(K(\bar\theta,\bar\varphi)\big)E^K(\theta,\varphi) \\
&= \int_0^1 (1-s)\mathrm{D}^2 a\big(K(\bar\theta,\bar\varphi) + sE^K(\theta,\varphi)\big)[E^K(\theta,\varphi), E^K(\theta,\varphi)]\, ds, \\
\Delta^2 H(\theta,\varphi) &:= H\big(\phi_T(K(\theta,\varphi),\varphi),\bar\varphi\big) - H\big(K(\bar\theta,\bar\varphi),\bar\varphi\big) - \mathrm{D}_z H\big(K(\bar\theta,\bar\varphi),\bar\varphi\big)E^K(\theta,\varphi) \\
&= \int_0^1 (1-s)\mathrm{D}_z^2 H\big(K(\bar\theta,\bar\varphi) + sE(\theta,\varphi),\bar\varphi\big)[E^K(\theta,\varphi), E^K(\theta,\varphi)]\, ds.
\end{aligned}$$

Proof. Let us start with $\langle \eta^{31} \rangle$ by using the exactness of the symplectic form as expressed in (4) to obtain

$$\langle \eta^{31} \rangle = \left\langle \mathrm{D}_\theta K(\bar\theta,\bar\varphi)^\top \mathrm{D}a\big(K(\bar\theta,\bar\varphi)\big)^\top E^K(\theta,\varphi) \right\rangle - \left\langle \mathrm{D}_\theta K(\bar\theta,\bar\varphi)^\top \mathrm{D}a\big(K(\bar\theta,\bar\varphi)\big)E^K(\theta,\varphi) \right\rangle.$$

We use that

$$\begin{aligned}
0 &= \left\langle \mathrm{D}_\theta \Big(a\big(K(\bar\theta,\bar\varphi)\big)^\top E^K(\theta,\varphi) \Big) \right\rangle \\
&= \left\langle E^K(\theta,\varphi)^\top \mathrm{D}_\theta\big(a\big(K(\bar\theta,\bar\varphi)\big)\big) + a\big(K(\bar\theta,\bar\varphi)\big)^\top \mathrm{D}_\theta E^K(\theta,\varphi) \right\rangle,
\end{aligned}$$

so we have

$$\langle \eta^{31} \rangle = -\left\langle \mathrm{D}_\theta E^K(\theta,\varphi)^\top a\big(K(\bar\theta,\bar\varphi)\big) + \mathrm{D}_\theta K(\bar\theta,\bar\varphi)^\top \big(\Delta^1 a(\theta,\varphi) - \Delta^2 a(\theta,\varphi)\big) \right\rangle.$$

We will now use

$$\begin{aligned}
\mathrm{D}_\theta E^K(\theta,\varphi) &= \mathrm{D}_z \phi_T\big(K(\theta,\varphi),\varphi\big)\mathrm{D}_\theta K(\theta,\varphi) - \mathrm{D}_\theta K(\bar\theta,\bar\varphi), \\
\left\langle \mathrm{D}_\theta K(\bar\theta,\bar\varphi)^\top a\big(K(\bar\theta,\bar\varphi)\big) \right\rangle &= \left\langle \mathrm{D}_\theta K(\theta,\varphi)^\top a\big(K(\theta,\varphi)\big) \right\rangle,
\end{aligned}$$

Eq. (6), and

$$\mathrm{D}_\theta\big(p_T(K(\theta,\varphi),\varphi)\big) = \Big(a\big(\phi_T(K(\theta,\varphi),\varphi)\big)^\top \mathrm{D}_z\phi_T(K(\theta,\varphi),\varphi) - a\big(K(\theta,\varphi)\big)^\top\Big)\mathrm{D}_\theta K(\theta,\varphi)$$

to rewrite $\langle \eta^{31}\rangle$ as

$$\begin{aligned}\big\langle \eta^{31}\big\rangle &= \big\langle \mathrm{D}_\theta E^K(\theta,\varphi)^\top \Delta^1 a(\theta,\varphi) + \mathrm{D}_\theta K(\bar\theta,\bar\varphi)^\top \Delta^2 a(\theta,\varphi)\big\rangle \\ &\quad - \Big\langle \mathrm{D}_\theta K(\theta,\varphi)^\top \Big(\mathrm{D}_z\phi_T\big(K(\theta,\varphi),\varphi\big)^\top a\big(\phi_T(K(\theta,\varphi),\varphi)\big) + a\big(K(\theta,\varphi)\big)\Big)\Big\rangle \\ &= \big\langle \mathrm{D}_\theta E^K(\theta,\varphi)^\top \Delta^1 a(\theta,\varphi) + \mathrm{D}_\theta K(\bar\theta,\bar\varphi)^\top \Delta^2 a(\theta,\varphi)\big\rangle - \Big\langle \mathrm{D}_\theta\big(p_T(K(\theta,\varphi),\varphi)\big)^\top\Big\rangle \\ &= \big\langle \mathrm{D}_\theta E^K(\theta,\varphi)^\top \Delta^1 a(\theta,\varphi) + \mathrm{D}_\theta K(\bar\theta,\bar\varphi)^\top \Delta^2 a(\theta,\varphi)\big\rangle\,,\end{aligned}$$

For η^{32}, we expand $\mathcal{X}_H$ to obtain

$$\big\langle \eta^{32}\big\rangle = \Big\langle X_H\big(K(\bar\theta,\bar\varphi),\bar\varphi\big)^\top \Omega\big(K(\bar\theta,\bar\varphi)E^K(\theta,\varphi)\Big\rangle - \big\langle \hat\alpha^\top \mathrm{D}_\varphi K(\bar\theta,\bar\varphi)^\top \Omega\big(K(\bar\theta,\bar\varphi)\big)E^K(\theta,\varphi)\big\rangle$$

and define

$$\begin{aligned}\eta^{32}_1(\theta,\varphi) &:= X_H\big(K(\bar\theta,\bar\varphi,\bar\varphi\big)^\top \Omega\big(K(\bar\theta,\bar\varphi)E^K(\theta,\varphi), \\ \eta^{32}_2(\theta,\varphi) &:= -\hat\alpha^\top \mathrm{D}_\varphi K(\bar\theta,\bar\varphi)^\top \Omega\big(K(\bar\theta,\bar\varphi)\big)E^K(\theta,\varphi)\end{aligned}$$

in order to inspect each term of η^{32} separately. We first use that $\mathrm{D}_z H(z,\varphi) = -X_H(z,\varphi)^\top\Omega(z)$ to express $\langle \eta^{32}_1\rangle$ as

$$\big\langle \eta^{32}_1\big\rangle = -\big\langle \mathrm{D}_z H\big(K(\bar\theta,\bar\varphi),\bar\varphi\big)E^K(\theta,\varphi)\big\rangle\,.$$

Hence,

$$\big\langle \eta^{32}_1\big\rangle = \big\langle \Delta^2 H(\theta,\varphi)\big\rangle - \big\langle H\big(\phi_T(K(\theta,\varphi),\varphi),\bar\varphi\big) - H\big(K(\theta,\varphi),\varphi\big)\big\rangle$$

where we used that

$$\big\langle H\big(K(\bar\theta,\bar\varphi),\bar\varphi\big)\big\rangle = \big\langle H\big(K(\theta,\varphi),\varphi\big)\big\rangle\,.$$

Let $R_t(\varphi) = \varphi + \hat\alpha t$. We use the fundamental theorem of calculus so

$$\begin{aligned}&H\Big(\phi_T\big(K(\theta,\varphi),\varphi\big),\bar\varphi\Big) - H\big(K(\theta,\varphi),\varphi\big) \\ &= \int_0^T \frac{d}{dt}\Big(H\Big(\phi_t\big(K(\theta,\varphi),\varphi\big),R_t(\varphi)\Big)\Big)dt \\ &= \int_0^T \Big(\mathrm{D}_z H\Big(\phi_t\big(K(\theta,\varphi),\varphi\big),R_t(\varphi)\Big)X_H\Big(\phi_t\big(K(\theta,\varphi),\varphi\big),R_t(\varphi)\Big)\Big)dt \\ &\quad + \int_0^T \Big(\mathrm{D}_\varphi H\Big(\phi_t\big(K(\theta,\varphi),\varphi\big),R_t(\varphi)\Big)\hat\alpha\Big)dt,\end{aligned}$$

where the first integral varnishes because

$$\mathrm{D}_z H(z,\varphi)X_H(z,\varphi) = -X_H(z,\varphi)^\top\Omega(z)X_H(z,\varphi) = 0.$$

Consequently,

$$\big\langle \eta^{32}_1\big\rangle = \big\langle \Delta^2 H(\theta,\varphi)\big\rangle - \Big\langle \int_0^T \Big(\mathrm{D}_\varphi H\Big(\phi_t\big(K(\theta,\varphi),\varphi\big),R_t(\varphi)\Big)\hat\alpha\Big)\ dt\Big\rangle\,.$$

We now use (8) to express $\langle \eta_1^{32} \rangle$ as

$$\begin{aligned}\left\langle \eta_1^{32} \right\rangle &= \left\langle \Delta^2 H(\theta,\varphi) \right\rangle - \left\langle a\Big(\phi_T\big(K(\theta,\varphi),\varphi\big)\Big)^\top \mathrm{D}_\varphi \phi_T\big(K(\theta,\varphi),\varphi\big)\hat\alpha - \mathrm{D}_\varphi p_T\big(K(\theta,\varphi),\varphi\big)\hat\alpha \right\rangle \\ &= \left\langle \Delta^2 H(\theta,\varphi) \right\rangle - \left\langle a\Big(\phi_T\big(K(\theta,\varphi),\varphi\big)\Big)^\top \mathrm{D}_\varphi \phi_T\big(K(\theta,\varphi),\varphi\big)\hat\alpha \right\rangle \\ &\quad - \left\langle \mathrm{D}_z p_T\big(K(\theta,\varphi),\varphi\big)\mathrm{D}_\varphi K(\theta,\varphi)\hat\alpha \right\rangle,\end{aligned}$$

where we used

$$0 = \left\langle \mathrm{D}_\varphi\Big(p_T\big(K(\theta,\varphi),\varphi\big)\Big) \right\rangle = \left\langle \mathrm{D}_z p_T\big(K(\theta,\varphi),\varphi\big)\mathrm{D}_\varphi K(\theta,\varphi) + \mathrm{D}_\varphi p_T\big(K(\theta,\varphi),\varphi\big) \right\rangle.$$

We then use that

$$\mathrm{D}_\varphi E^K(\theta,\varphi) = \mathrm{D}_z \phi_T\big(K(\theta,\varphi),\varphi\big)\mathrm{D}_\varphi K(\theta,\varphi) + \mathrm{D}_\varphi \phi_T\big(K(\theta,\varphi),\varphi\big) - \mathrm{D}_\varphi K(\bar\theta,\bar\varphi),$$

in order to rewrite $\langle \eta_1^{32} \rangle$ as

$$\begin{aligned}\left\langle \eta_1^{32} \right\rangle &= \left\langle \Delta^2 H(\theta,\varphi) \right\rangle - \left\langle a\Big(\phi_T\big(K(\theta,\varphi),\varphi\big)\Big)^\top \mathrm{D}_\varphi E^K(\theta,\varphi)\hat\alpha \right\rangle \\ &\quad + \left\langle a\Big(\phi_T\big(K(\theta,\varphi),\varphi\big)\Big)^\top \mathrm{D}_z \phi_T\big(K(\theta,\varphi,\varphi)\big)\mathrm{D}_\varphi K(\theta,\varphi)\hat\alpha \right\rangle \\ &\quad - \left\langle a\Big(\phi_T\big(K(\theta,\varphi),\varphi\big)\Big)^\top \mathrm{D}_\varphi K(\bar\theta,\bar\varphi)\hat\alpha \right\rangle \\ &\quad - \left\langle \mathrm{D}_z p_T\big(K(\theta,\varphi),\varphi\big)\mathrm{D}_\varphi K(\theta,\varphi)\hat\alpha \right\rangle \\ &= \left\langle \Delta^2 H(\theta,\varphi) \right\rangle - \left\langle a\Big(\phi_T\big(K(\theta,\varphi),\varphi\big)\Big)^\top \mathrm{D}_\varphi K(\bar\theta,\bar\varphi)\hat\alpha \right\rangle \\ &\quad - \left\langle a\Big(\phi_T\big(K(\theta,\varphi),\varphi\big)\Big)^\top \mathrm{D}_\varphi E^K(\theta,\varphi)\hat\alpha - a\big(K(\bar\theta,\bar\varphi)\big)^\top \mathrm{D}_\varphi K(\bar\theta,\bar\varphi)\hat\alpha \right\rangle,\end{aligned}$$

where we used Eq. (6) in the last equality and that

$$\left\langle a\big(K(\theta,\varphi)\big)^\top \mathrm{D}_\varphi K(\theta,\varphi)\hat\alpha \right\rangle = \left\langle a\big(K(\bar\theta,\bar\varphi)\big)^\top \mathrm{D}_\varphi K(\bar\theta,\bar\varphi)\hat\alpha \right\rangle.$$

We leave the term η_1^{32} as it is. For the term η_2^{32}, we use (4) to obtain

$$\left\langle \eta_2^{32} \right\rangle = \left\langle \hat\alpha^\top \mathrm{D}_\varphi K(\bar\theta,\bar\varphi)^\top \mathrm{D}a\big(K(\bar\theta,\bar\varphi)\big)E^K(\theta,\varphi) \right\rangle - \left\langle \hat\alpha^\top \mathrm{D}_\varphi K(\bar\theta,\bar\varphi)^\top \mathrm{D}a\big(K(\bar\theta,\bar\varphi)\big)^\top E^K(\theta,\varphi) \right\rangle$$

Then, we use that

$$\begin{aligned}0 &= \left\langle \mathrm{D}_\varphi\Big(a\big(K(\bar\theta,\bar\varphi)\big)^\top E^K(\theta,\varphi)\Big) \right\rangle \\ &= \left\langle E^K(\theta,\varphi)^\top \mathrm{D}_\varphi\Big(a\big(K(\bar\theta,\bar\varphi)\big)\Big) + a\big(K(\bar\theta,\bar\varphi)\big)^\top \mathrm{D}_\varphi E^K(\theta,\varphi) \right\rangle\end{aligned}$$

and the definitions for $\Delta^1 a$ and $\Delta^2 a$ to obtain

$$\left\langle \eta_2^{32} \right\rangle = \left\langle a\big(K(\bar\theta,\bar\varphi)\big)^\top \mathrm{D}_\varphi E^K(\theta,\varphi)\hat\alpha \right\rangle + \left\langle \Big(\Delta^1 a(\theta,\varphi)^\top - \Delta^2 a(\theta,\varphi)^\top\Big)\mathrm{D}_\varphi K(\bar\theta,\bar\varphi)\hat\alpha \right\rangle,$$

where we used that $\eta_2^{32} = \left(\eta_2^{32}\right)^\top$ since η_2^{32} is a scalar. Lastly, we obtain $\langle \eta^{32} \rangle$ as

$$\begin{aligned}
\left\langle \eta^{32} \right\rangle &= \left\langle \eta_1^{32} \right\rangle + \left\langle \eta_2^{32} \right\rangle \\
&= \left\langle \Delta^2 H(\theta,\varphi) \right\rangle - \left\langle a\Big(\phi_T\big(K(\theta,\varphi),\varphi\big)\Big)^\top \mathrm{D}_\varphi E^K(\theta,\varphi)\hat\alpha - a\big(K(\bar\theta,\bar\varphi)\big)^\top \mathrm{D}_\varphi K(\bar\theta,\bar\varphi)\hat\alpha \right\rangle \\
&\quad - \left\langle a\Big(\phi_T\big(K(\theta,\varphi),\varphi\big)\Big)^\top \mathrm{D}_\varphi K(\bar\theta,\bar\varphi)\hat\alpha \right\rangle \\
&\quad + \left\langle a\big(K(\bar\theta,\bar\varphi)\big)^\top \mathrm{D}_\varphi E^K(\theta,\varphi)\hat\alpha + \Delta^1 a(\theta,\varphi)^\top \mathrm{D}_\varphi K(\bar\theta,\bar\varphi)\hat\alpha \right\rangle \\
&\quad - \left\langle \Delta^2 a(\theta,\varphi)^\top \mathrm{D}_\varphi K(\bar\theta,\bar\varphi)\hat\alpha \right\rangle \\
&= \left\langle \Delta^2 H(\theta,\varphi) \right\rangle - \left\langle \Delta^1 a(\theta,\varphi)^\top \mathrm{D}_\varphi E^K(\theta,\varphi)\hat\alpha \right\rangle - \left\langle \Delta^2 a(\theta,\varphi)^\top \mathrm{D}_\varphi K(\bar\theta,\bar\varphi)\hat\alpha \right\rangle .
\end{aligned}$$

□

Appendix B. Fiberwise symplectic deformations and moment maps

In this section we introduce the notion of fiberwise symplectic deformations and establish their main properties. For a general exposition on symplectic deformations see [GHdlL14].

Definition B.1. *A fiberwise symplectic deformation in $U \subset \mathbb{R}^{2n}$ and with base $G \subset \mathbb{R}^m$ is a smooth diffeomorphism*

$$\begin{aligned}
\Phi : \quad & U \times G \longrightarrow U \times G \\
& (z, \boldsymbol{t}) \longmapsto \big(\phi_{\boldsymbol{t}}(z), \tau(\boldsymbol{t})\big),
\end{aligned}$$

such that for all $\boldsymbol{t} \in G$, $\phi_{\boldsymbol{t}} : U \to U$ is symplectic and $\tau : G \to G$ is the base of the deformation. If for all $\boldsymbol{t} \in G$, $\phi_{\boldsymbol{t}}(z) = \phi(z, \boldsymbol{t})$ is exact symplectic, we will say that the fiberwise deformation is Hamiltonian.

Definition B.2. *The primitive function of a fiberwise Hamiltonian deformation $\Phi : U \times G \to U \times G$ is a smooth function $p : U \times G \to \mathbb{R}$ such that for all $\boldsymbol{t} \in G$, the function $p_{\boldsymbol{t}}(z) = p(z, \boldsymbol{t})$ is the primitive function of $\phi_{\boldsymbol{t}}(z)$.*

Definition B.3. *Let $\Phi : U \times G \to U \times G$ be a fiberwise Hamiltonian deformation and let $p : U \times G \to \mathbb{R}$ be the primitive function of Φ.*

(i) *The generator of Φ is the function $\mathcal{F} : U \times G \to \mathbb{R}^{2n\times m}$ defined as*

$$\mathcal{F}_{\boldsymbol{t}}(z) := \mathrm{D}_{\boldsymbol{t}}\phi\big(\phi^{-1}_{\tau^{-1}(\boldsymbol{t})}(z), \tau^{-1}(\boldsymbol{t})\big), \tag{70}$$

where $\mathcal{F}_{\boldsymbol{t}}(z) = \mathcal{F}(z,\boldsymbol{t}) = \Big(\mathcal{F}^1(z,\boldsymbol{t}) \;\; \mathcal{F}^2(z,\boldsymbol{t}) \;\; \dots \;\; \mathcal{F}^m(z,\boldsymbol{t})\Big)$.

(ii) *The moment map of Φ is the function $\mathcal{M} : U \times G \to \mathbb{R}^m$ defined as*

$$\mathcal{M}_{\boldsymbol{t}}(z)^\top := a(z)^\top \mathcal{F}_{\boldsymbol{t}}(z) - \mathrm{D}_{\boldsymbol{t}} p\big(\phi^{-1}_{\tau^{-1}(\boldsymbol{t})}(z), \tau^{-1}(\boldsymbol{t})\big),$$

where $\mathcal{M}_{\boldsymbol{t}}(z) = \mathcal{M}(z,\boldsymbol{t}) = \Big(\mathcal{M}^1(z,\boldsymbol{t}) \ \mathcal{M}^2(z,\boldsymbol{t}) \ \ldots \ \mathcal{M}^m(z,\boldsymbol{t})\Big)^\top$.

Lemma B.4. *For all* $\boldsymbol{t} \in G$, *the moment map* $\mathcal{M}$ *satisfies*

$$\mathcal{F}_{\boldsymbol{t}}(z) = \Omega(z)^{-1}\big(\mathrm{D}_z\mathcal{M}_{\boldsymbol{t}}(z)\big)^\top.$$

Proof. For $i = 1, 2, \ldots, m$, let us differentiate $\mathcal{M}^i\big(\phi_{\boldsymbol{t}}(z), \tau(\boldsymbol{t})\big)$ with respect to z as

$$\begin{aligned}
\mathrm{D}_z\Big(\mathcal{M}^i\big(\phi_{\boldsymbol{t}}(z),\tau(\boldsymbol{t})\big)\Big) &= \mathrm{D}_z\Big(a\big(\phi_{\boldsymbol{t}}(z)\big)^\top\partial_{t_i}\phi_{\boldsymbol{t}}(z) - \partial_{t_i}p_{\boldsymbol{t}}(z)\Big)\\
&= a\big(\phi_{\boldsymbol{t}}(z)\big)^\top\partial_{t_i}\mathrm{D}_z\phi_t(z) + \partial_{t_i}\phi_{\boldsymbol{t}}(z)^\top\mathrm{D}a\big(\phi_{\boldsymbol{t}}(z)\big)\mathrm{D}_z\phi_{\boldsymbol{t}}(z)\\
&\quad - \partial_{t_i}\Big(a\big(\phi_{\boldsymbol{t}}(z)\big)^\top\mathrm{D}_z\phi_{\boldsymbol{t}}(z) - a(z)^\top\Big)\\
&= a\big(\phi_{\boldsymbol{t}}(z)\big)^\top\partial_{t_i}\mathrm{D}_z\phi_{\boldsymbol{t}}(z) + \partial_{t_i}\phi_{\boldsymbol{t}}(z)^\top\mathrm{D}a\big(\phi_{\boldsymbol{t}}(z)\big)\mathrm{D}_z\phi_{\boldsymbol{t}}(z)\\
&\quad - a\big(\phi_{\boldsymbol{t}}(z)\big)^\top\partial_{t_i}\mathrm{D}_z\phi_{\boldsymbol{t}}(z) - \partial_{t_i}\phi_{\boldsymbol{t}}(z)^\top\mathrm{D}a\big(\phi_{\boldsymbol{t}}(z)\big)^\top\mathrm{D}_z\phi_{\boldsymbol{t}}(z)\\
&= -\partial_{t_i}\phi_{\boldsymbol{t}}(z)^\top\Omega\big(\phi_{\boldsymbol{t}}(z)\big)\mathrm{D}_z\phi_{\boldsymbol{t}}(z).
\end{aligned}$$

On the other hand, applying the chain rule we also have

$$\mathrm{D}_z\Big(\mathcal{M}^i\big(\phi_{\boldsymbol{t}}(z),\tau(\boldsymbol{t})\big)\Big) = \mathrm{D}_z\mathcal{M}^i\big(\phi_{\boldsymbol{t}}(z),\tau(\boldsymbol{t})\big)\mathrm{D}_z\phi_{\boldsymbol{t}}(z).$$

Assuming that $\mathrm{D}_z\phi_{\boldsymbol{t}}(z)$ is invertible, we obtain

$$\mathrm{D}_z\mathcal{M}^i\big(\phi_{\boldsymbol{t}}(z),\tau(\boldsymbol{t})\big) = -\partial_{t_i}\phi_{\boldsymbol{t}}(z)^\top\Omega\big(\phi_{\boldsymbol{t}}(z)\big),$$

and evaluating at $\bar{z} = \phi^{-1}_{\tau^{-1}(\boldsymbol{t})}(z)$ and $\bar{\boldsymbol{t}} = \tau^{-1}(\boldsymbol{t})$,

$$\mathrm{D}_z\mathcal{M}^i(z,\boldsymbol{t}) = -\partial_{t_i}\phi\big(\phi^{-1}_{\tau^{-1}(\boldsymbol{t})}(z),\tau^{-1}(\boldsymbol{t})\big)^\top\Omega(z).$$

Equivalently, using the definition of the generator given by (70), we conclude

$$\mathcal{F}^i(z,\boldsymbol{t}) = \Omega(z)^{-1}\big(\mathrm{D}_z\mathcal{M}^i(z,\boldsymbol{t})\big)^\top$$

□

Remark B.5. *Note that, for* $i = 1, ..., m$, *the moment map* $\mathcal{M}$ *gives the Hamiltonian* $\mathcal{M}^i$ *for the vector field* $\mathcal{F}^i$ *obtained by differentiating* $\phi_{\boldsymbol{t}}$ *with respect to* t_i.

In the context of the present paper, let us consider flows of a quasi-periodic Hamiltonian system, defined by the function H, with frequencies $\hat{\alpha} \in \mathbb{R}^\ell$. As described in Section 2, for each (z,φ) the flow $\tilde{\phi} : I_{z,\varphi} \times U \times \mathbb{T}^\ell \to U \times \mathbb{T}^\ell$, where $I_{z,\varphi} \subset \mathbb{R}$ is the maximal interval of existence for initial conditions (z,φ), adopts the form

$$\tilde{\phi}_t(z,\varphi) = \begin{pmatrix}\phi_t(z,\varphi)\\ \varphi + \hat{\alpha}t\end{pmatrix},$$

where the evolution operator ϕ_t is fiberwise exact symplectic for all $t \in I_{z,\varphi}$. Let us first define the rotation operator $R_t(\varphi) := \varphi + \hat{\alpha}t$. We observe that for fixed t, and each (z,φ), we can identify time-t maps with fiberwise Hamiltonian deformations $\Phi : U\times G \to U\times G$

$$\begin{aligned}\Phi:\quad U\times G &\longrightarrow U\times G\\ (z,\boldsymbol{t}) &\longmapsto \big(\phi_t(z,\varphi),\tau(\boldsymbol{t})\big),\end{aligned}$$

where $G\subset\mathbb{R}^{\ell+1}$, $\boldsymbol{t}=(t,\varphi)$, and $\tau(\boldsymbol{t})=\big(t,R_t(\varphi)\big)$. For a quasi-periodic Hamiltonian $H_\varepsilon(z,\varphi)$ that depends on some parameter $\varepsilon\in\mathbb{R}$, we can again identify time-t maps with fiberwise Hamiltonian deformations $\Phi : U\times G\to U\times G$

$$\begin{aligned}\Phi:\quad U\times G &\longrightarrow U\times G\\ (z,\boldsymbol{t}) &\longmapsto \big(\phi_{t,\varepsilon}(z,\varphi),\tau(\boldsymbol{t})\big),\end{aligned}$$

where $G\subset\mathbb{R}^{\ell+2}$, $\boldsymbol{t}=(t,\varepsilon,\varphi)$, and $\tau(\boldsymbol{t})=\big(t,\varepsilon,R_t(\varphi)\big)$. We will also write $\Phi_{\boldsymbol{t}}(z)=\Phi_{t,\varepsilon}(z,\varphi)$.

Lemma B.6. *The moment map of $\Phi_{t,\varepsilon}(z,\varphi)$ is given by*

$$\begin{aligned}\mathcal{M}^t\big(\phi_{t,\varepsilon}(z,\varphi),\tau(\boldsymbol{t})\big) &= H_\varepsilon\big(\phi_{t,\varepsilon}(z,\varphi),R_t(\varphi)\big)\\ \mathcal{M}^\varepsilon\big(\phi_{t,\varepsilon}(z,\varphi),\tau(\boldsymbol{t})\big) &= \int_0^t \partial_\varepsilon H_\varepsilon\big(\phi_{s,\varepsilon}(z,\varphi),R_s(\varphi)\big)\,ds\\ \mathcal{M}^\varphi\big(\phi_{t,\varepsilon}(z,\varphi),\tau(\boldsymbol{t})\big) &= \int_0^t \mathrm{D}_\varphi H_\varepsilon\big(\phi_{s,\varepsilon}(z,\varphi),R_s(\varphi)\big)\,ds\end{aligned}$$

Proof. For $\mathcal{M}^t\big(\phi_{t,\varepsilon}(z,\varphi),\tau(\boldsymbol{t})\big)$, let us use the definition of the moment map and the primitive function of ϕ_t as given in (7)—which, for each (t,ε,φ), coincides with the primitive function of the fiberwise Hamiltonian deformation $\Phi_{t,\varepsilon}(z,\varphi)$—to obtain

$$\begin{aligned}\mathcal{M}^t\big(\phi_{t,\varepsilon}(z,\varphi),\tau(\boldsymbol{t})\big) &= a\big(\phi_{t,\varepsilon}(z,\varphi)\big)^\top\partial_t\phi_{t,\varepsilon}(z,\varphi)-\partial_t p_{t,\varepsilon}(z,\varphi)\\ &= a\big(\phi_{t,\varepsilon}(z,\varphi)\big)^\top X_{H_\varepsilon}\big(\phi_{t,\varepsilon}(z,\varphi),R_t(\varphi)\big)\\ &\quad - a\big(\phi_{t,\varepsilon}(z,\varphi)\big)^\top X_{H_\varepsilon}\big(\phi_{t,\varepsilon}(z,\varphi),R_t(\varphi)\big)+H_\varepsilon\big(\phi_{t,\varepsilon}(z,\varphi),R_t(\varphi)\big)\\ &= H_\varepsilon\big(\phi_{t,\varepsilon}(z,\varphi),R_t(\varphi)\big).\end{aligned}$$

Note that this result could have been obtained directly from Remark B.5.

For $\mathcal{M}^\varepsilon\big(\phi_{t,\varepsilon}(z,\varphi),\tau(\boldsymbol{t})\big)$, let us first differentiate the primitive function of Φ with respect to ε

$$\begin{aligned}\partial_\varepsilon p_{t,\varepsilon}(z,\varphi) &= \partial_\varepsilon\left(\int_0^t\Big(a\big(\phi_{s,\varepsilon}(z,\varphi)\big)^\top X_{H_\varepsilon}\big(\phi_{s,\varepsilon}(z,\varphi),R_s(\varphi)\big)-H_\varepsilon\big(\phi_{s,\varepsilon}(z,\varphi),R_s(\varphi)\big)\Big)ds\right)\\ &= \int_0^t\Big(X_{H_\varepsilon}\big(\phi_{s,\varepsilon}(z,\varphi),R_s(\varphi)\big)^\top \mathrm{D}a\big(\phi_{s,\varepsilon}(z,\varphi)\big)\partial_\varepsilon\phi_{s,\varepsilon}(z,\varphi)\\ &\quad + a\big(\phi_{s,\varepsilon}(z,\varphi)\big)^\top\Big(\mathrm{D}_zX_{H_\varepsilon}\big(\phi_{s,\varepsilon}(z,\varphi),R_s(\varphi)\big)\partial_\varepsilon\phi_{s,\varepsilon}(z,\varphi)\\ &\quad + \partial_\varepsilon X_{H_\varepsilon}\big(\phi_{s,\varepsilon}(z,\varphi),R_s(\varphi)\big)\Big)-\mathrm{D}_zH_\varepsilon\big(\phi_{s,\varepsilon}(z,\varphi),R_s(\varphi)\big)\partial_\varepsilon\phi_{s,\varepsilon}(z,\varphi)\\ &\quad - \partial_\varepsilon H_\varepsilon\big(\phi_{s,\varepsilon}(z,\varphi),R_s(\varphi)\big)\Big)\ ds.\end{aligned}$$

We use that $\mathrm{D}_zH_\varepsilon(z,\varphi)=-X_{H_\varepsilon}^\top(z,\varphi)\Omega(z)$ and (4) to obtain

$$\begin{aligned}\partial_\varepsilon p_{t,\varepsilon}(z,\varphi) &= \int_0^t\Big(X_{H_\varepsilon}\big(\phi_{s,\varepsilon}(z,\varphi),R_s(\varphi)\big)^\top \mathrm{D}a\big(\phi_{s,\varepsilon}(z,\varphi)\big)^\top\partial_\varepsilon\phi_{s,\varepsilon}(z,\varphi)\\ &\quad + a\big(\phi_{s,\varepsilon}(z,\varphi)\big)^\top\Big(\mathrm{D}_zX_{H_\varepsilon}\big(\phi_{s,\varepsilon}(z,\varphi),R_s(\varphi)\big)\partial_\varepsilon\phi_{s,\varepsilon}(z,\varphi)\\ &\quad + \partial_\varepsilon X_{H_\varepsilon}\big(\phi_{s,\varepsilon}(z,\varphi),R_s(\varphi)\big)\Big)-\partial_\varepsilon H_\varepsilon\big(\phi_{s,\varepsilon}(z,\varphi),R_s(\varphi)\big)\Big)ds,\end{aligned}$$

which we can rewrite as

$$\begin{aligned}\partial_\varepsilon p_{t,\varepsilon}(z,\varphi) &= \int_0^t\left(\frac{d}{ds}\Big(a\big(\phi_{s,\varepsilon}(z,\varphi)\big)\Big)^\top\partial_\varepsilon\phi_{s,\varepsilon}(z,\varphi)+a\big(\phi_{s,\varepsilon}(z,\varphi)\big)^\top\frac{d}{ds}\big(\partial_\varepsilon\phi_{s,\varepsilon}(z,\varphi)\big)\right.\\ &\quad \left.-\,\partial_\varepsilon H_\varepsilon\big(\phi_{s,\varepsilon}(z,\varphi),R_s(\varphi)\big)\right)ds\end{aligned}$$

and obtain

$$\begin{aligned}\partial_\varepsilon p_{t,\varepsilon}(z,\varphi) &= \int_0^t\left(\frac{d}{ds}\Big(a\big(\phi_{s,\varepsilon}(z,\varphi)\big)^\top\partial_\varepsilon\phi_{s,\varepsilon}(z,\varphi)\Big)-\partial_\varepsilon H_\varepsilon\big(\phi_{s,\varepsilon}(z,\varphi),R_s(\varphi)\big)\right)ds\\ &= a\big(\phi_{t,\varepsilon}(z,\varphi)\big)^\top\partial_\varepsilon\phi_{t,\varepsilon}(z,\varphi)-\int_0^t\partial_\varepsilon H_\varepsilon\big(\phi_{s,\varepsilon}(z,\varphi),R_s(\varphi)\big)ds.\end{aligned}$$

Then, by definition, we have

$$\begin{aligned}\mathcal{M}^\varepsilon\big(\phi_{t,\varepsilon}(z,\varphi),\tau(\boldsymbol{t})\big) &= a\big(\phi_{t,\varepsilon}(z,\varphi)\big)^\top\partial_\varepsilon\phi_{t,\varepsilon}(z,\varphi)-\partial_\varepsilon p_{t,\varepsilon}(z,\varphi)\\ &= \int_0^t\partial_\varepsilon H_\varepsilon\big(\phi_{s,\varepsilon}(z,\varphi),R_s(\varphi)\big)\ ds.\end{aligned}$$

For $\mathcal{M}^\varphi\big(\phi_{t,\varepsilon}(z,\varphi),\tau(\boldsymbol{t})\big)$, we will use the the expression of $\mathrm{D}_\varphi p_t$ given by (8). Then for the primitive function of Φ, we have

$$\mathrm{D}_\varphi p_{t,\varepsilon}(z,\varphi)=a\big(\phi_{t,\varepsilon}(z,\varphi)\big)^\top\mathrm{D}_\varphi\phi_{t,\varepsilon}(z,\varphi)-\int_0^t\Big(\mathrm{D}_\varphi H_\varepsilon\big(\phi_{s,\varepsilon}(z,\varphi),R_s(\varphi)\big)\Big)ds.$$

Hence,

$$\begin{aligned}\mathcal{M}^{\varphi}\big(\phi_{t,\varepsilon}(z,\varphi),\tau(\boldsymbol{t})\big) &= a\big(\phi_{t,\varepsilon}(z,\varphi)\big)^{\top}\mathrm{D}_{\varphi}\phi_{t,\varepsilon}(z,\varphi) - \mathrm{D}_{\varphi}p_{t,\varepsilon}(z,\varphi)\\ &= \int_0^t \mathrm{D}_{\varphi}H_{\varepsilon}\big(\phi_{s,\varepsilon}(z,\varphi),R_s(\varphi)\big)\,ds.\end{aligned}$$

Note that it is possible to obtain expressions for $\mathcal{M}(z,\mathbf{t})$, but we provide here the expressions for $\mathcal{M}\big(\phi_{t,\varepsilon}(z,\varphi),\tau(\boldsymbol{t})\big)$ since they will be useful in the next section.

□

Appendix C. Zero averages

For the continuation of an invariant torus $\mathcal{K}$ with respect to parameters of the Hamiltonian we need the averages of η^3 given by

$$\eta^3(\theta,\varphi) = \begin{pmatrix}\mathrm{D}_{\theta}K(\bar\theta,\bar\varphi)^{\top}\Omega\big(K(\bar\theta,\bar\varphi)\big)\partial_{\varepsilon}\phi_{T,\varepsilon}\big(K(\theta,\varphi),\varphi\big)\\ \mathcal{X}_H(\bar\theta,\bar\varphi)^{\top}\Omega\big(K(\bar\theta,\bar\varphi)\big)\partial_{\varepsilon}\phi_{T,\varepsilon}\big(K(\theta,\varphi),\varphi\big)\end{pmatrix}$$

to be zero in order for the small divisors cohomological equations from Section 3.3 to be solvable. Recall the definitions $\bar\theta := \theta+\omega$ and $\bar\varphi = \varphi+\alpha$, and let us define

$$\begin{pmatrix}\eta^{31}(\theta,\varphi)\\ \eta^{32}(\theta,\varphi)\end{pmatrix} := \begin{pmatrix}\mathrm{D}_{\theta}K(\bar\theta,\bar\varphi)^{\top}\Omega\big(K(\bar\theta,\bar\varphi)\big)\partial_{\varepsilon}\phi_{T,\varepsilon}\big(K(\theta,\varphi),\varphi\big)\\ \mathcal{X}_H(\bar\theta,\bar\varphi)^{\top}\Omega\big(K(\bar\theta,\bar\varphi)\big)\partial_{\varepsilon}\phi_{T,\varepsilon}\big(K(\theta,\varphi),\varphi\big)\end{pmatrix}.$$

Lemma C.1. *The averages of η^{31} and η^{32} are zero.*

Proof. Let us consider the following fiberwise Hamiltonian deformation $\Phi_{T,\varepsilon} : U\times G \to U\times G$

$$\begin{aligned}\Phi :\quad U\times G &\longrightarrow U\times G\\ (z,\boldsymbol{t}) &\longmapsto \big(\phi_{T,\varepsilon}(z,\varphi),\tau(\boldsymbol{t})\big),\end{aligned}$$

with $G\subset\mathbb{R}^{\ell+2}$, $\boldsymbol{t} = (T,\varepsilon,\varphi)$, and $\tau(\boldsymbol{t}) = \big(T,\varepsilon,\bar\varphi\big)$, see Appendix B. We can then use the definition of the generator $\mathcal{F}^{\varepsilon}$ of the fiberwise Hamiltonian deformation as given in (70), the invariance of $\mathcal{K}$ and Lemma B.4, and obtain for $\langle\eta^{31}\rangle$

$$\begin{aligned}\langle\eta^{31}\rangle &= \Big\langle \mathrm{D}_{\theta}K(\bar\theta,\bar\varphi)^{\top}\Omega\big(K(\bar\theta,\bar\varphi)\big)\mathcal{F}^{\varepsilon}_{T,\varepsilon}\Big(\phi_{T,\varepsilon}\big(K(\theta,\varphi),\varphi\big),\bar\varphi\Big)\Big\rangle\\ &= \big\langle \mathrm{D}_{\theta}K(\bar\theta,\bar\varphi)^{\top}\Omega\big(K(\bar\theta,\bar\varphi)\big)\mathcal{F}^{\varepsilon}_{T,\varepsilon}\big(K(\bar\theta,\bar\varphi),\bar\varphi\big)\big\rangle\\ &= \Big\langle \mathrm{D}_{\theta}K(\bar\theta,\bar\varphi)^{\top}\mathrm{D}_z\mathcal{M}^{\varepsilon}_{T,\varepsilon}\big(K(\bar\theta,\bar\varphi),\bar\varphi\big)^{\top}\Big\rangle\\ &= \Big\langle \mathrm{D}_{\theta}\Big(\mathcal{M}^{\varepsilon}_{T,\varepsilon}\big(K(\bar\theta,\bar\varphi),\bar\varphi\big)\Big)^{\top}\Big\rangle\\ &= 0\end{aligned}$$

since we are taking averages of derivatives with respect to θ.

For $\langle\eta^{32}\rangle$, let us use Lemma B.4 and that

$$\mathrm{D}_z\phi_{T,\varepsilon}\big(K(\theta,\varphi),\varphi\big)\mathcal{X}_H(\theta,\varphi) = \mathcal{X}_H(\bar\theta,\bar\varphi)$$

to rewrite $\langle \eta^{32} \rangle$ as

$$\langle \eta^{32} \rangle = \left\langle \mathcal{X}_H(\theta,\varphi)^\top \mathrm{D}_z \left(\mathcal{M}^{\varepsilon}_{T,\varepsilon}\Big(\phi_{T,\varepsilon}\big(K(\theta,\varphi),\varphi\big),\bar{\varphi}\Big) \right)^\top \right\rangle .$$

Let us transpose the previous expression and use the explicit form of $\mathcal{M}^{\varepsilon}_{T,\varepsilon}$ as given in Lemma B.6. Hence, using the rotation operator $R_s(\varphi) = \varphi + \hat{\alpha} s$, we have

$$\langle \eta^{32} \rangle = \left\langle \int_0^T \Big(\mathrm{D}_z \partial_\varepsilon H_\varepsilon\big(\phi_{s,\varepsilon}\big(K(\theta,\varphi),\varphi\big), R_s(\varphi)\big) \mathrm{D}_z \phi_{s,\varepsilon}\big(K(\theta,\varphi),\varphi\big) \mathcal{X}_H(\theta,\varphi) \Big) \, ds \right\rangle .$$

We then expand $\mathcal{X}_H$ to rewrite $\langle \eta^{32} \rangle$ as

$$\begin{aligned} \langle \eta^{32} \rangle = \Bigg\langle \int_0^T \Big(& \mathrm{D}_z \partial_\varepsilon H_\varepsilon\Big(\phi_{s,\varepsilon}\big(K(\theta,\varphi),\varphi\big), R_s(\varphi)\Big) \mathrm{D}_z \phi_{s,\varepsilon}\big(K(\theta,\varphi),\varphi\big) \\ & \Big(X_{H_\varepsilon}\big(K(\theta,\varphi),\varphi\big) - \mathrm{D}_\varphi K(\theta,\varphi)\hat{\alpha} \Big) \Big) \, ds \Bigg\rangle \end{aligned}$$

and we use that

$$X_{H_\varepsilon}\big(\phi_{t,\varepsilon}(z,\varphi), R_t(\varphi)\big) = \mathrm{D}_z \phi_{t,\varepsilon}(z,\varphi) X_{H_\varepsilon}(z,\varphi) + \mathrm{D}_\varphi \phi_{t,\varepsilon}(z,\varphi)\hat{\alpha},$$

see Section 3.1, to obtain

$$\begin{aligned} \langle \eta^{32} \rangle = \Bigg\langle \int_0^T \Big(& \mathrm{D}_z \partial_\varepsilon H_\varepsilon\Big(\phi_{s,\varepsilon}\big(K(\theta,\varphi),\varphi\big), R_s(\varphi)\Big) \frac{d}{ds}\Big(\phi_{s,\varepsilon}\big(K(\theta,\varphi),\varphi\big)\Big) \\ & - \mathrm{D}_z \partial_\varepsilon H_\varepsilon\Big(\phi_{s,\varepsilon}\big(K(\theta,\varphi),\varphi\big), R_s(\varphi)\Big) \mathrm{D}_z \phi_{s,\varepsilon}\big(K(\theta,\varphi),\varphi\big) \mathrm{D}_\varphi K(\theta,\varphi)\hat{\alpha} \\ & - \mathrm{D}_z \partial_\varepsilon H_\varepsilon\Big(\phi_{s,\varepsilon}\big(K(\theta,\varphi),\varphi\big), R_s(\varphi)\Big) \mathrm{D}_\varphi \phi_{s,\varepsilon}\big(K(\theta,\varphi),\varphi\big)\hat{\alpha} \Big) ds \Bigg\rangle. \end{aligned}$$

We can then rewrite it as

$$\begin{aligned} \langle \eta^{32} \rangle = \Bigg\langle \int_0^T \Big(& \mathrm{D}_z \partial_\varepsilon H_\varepsilon\Big(\phi_{s,\varepsilon}\big(K(\theta,\varphi),\varphi\big), R_s(\varphi)\Big) \frac{d}{ds}\Big(\phi_{s,\varepsilon}\big(K(\theta,\varphi),\varphi\big)\Big) \\ & + \mathrm{D}_\varphi \partial_\varepsilon H_\varepsilon\Big(\phi_{s,\varepsilon}\big(K(\theta,\varphi),\varphi\big), R_s(\varphi)\Big)\hat{\alpha} + \mathrm{D}_\varphi \partial_\varepsilon H_\varepsilon\Big(\phi_{s,\varepsilon}\big(K(\theta,\varphi),\varphi\big), R_s(\varphi)\Big)\hat{\alpha} \\ & - \mathrm{D}_z \partial_\varepsilon H_\varepsilon\Big(\phi_{s,\varepsilon}\big(K(\theta,\varphi),\varphi\big), R_s(\varphi)\Big) \mathrm{D}_z \phi_{s,\varepsilon}\big(K(\theta,\varphi),\varphi\big) \mathrm{D}_\varphi K(\theta,\varphi)\hat{\alpha} \\ & - \mathrm{D}_z \partial_\varepsilon H_\varepsilon\Big(\phi_{s,\varepsilon}\big(K(\theta,\varphi),\varphi\big), R_s(\varphi)\Big) \mathrm{D}_\varphi \phi_{s,\varepsilon}\big(K(\theta,\varphi),\varphi\big)\hat{\alpha} \Big) ds \Bigg\rangle \end{aligned}$$

to finally obtain

$$\begin{aligned}\langle \eta^{32} \rangle &= \left\langle \int_0^T -\mathrm{D}_\varphi \Big(\partial_\varepsilon H_\varepsilon \big(\phi_{s,\varepsilon}\big(K(\theta,\varphi),\varphi\big), R_s(\varphi) \big) \Big)\, ds \right\rangle \hat{\alpha} \\ &\quad + \left\langle \int_0^T \frac{d}{ds} \Big(\partial_\varepsilon H_\varepsilon \big(\phi_{s,\varepsilon}\big(K(\theta,\varphi),\varphi\big), R_s(\varphi) \big) \Big)\, ds \right\rangle \\ &= \left\langle -\mathrm{D}_\varphi \Big(\mathcal{M}^{\varepsilon}_{T,\varepsilon} \big(\phi_{T,\varepsilon}\big(K(\theta,\varphi),\varphi\big), \bar{\varphi} \big) \Big) \right\rangle \hat{\alpha} \\ &\quad + \big\langle \partial_\varepsilon H_\varepsilon \big(K(\bar{\theta},\bar{\varphi}),\bar{\varphi}\big) - \partial_\varepsilon H_\varepsilon\big(K(\theta,\varphi),\varphi\big) \big\rangle \\ &= 0,\end{aligned}$$

where we used that $\partial_\varepsilon H_\varepsilon\big(K(\theta,\varphi),\varphi\big)$ and $\partial_\varepsilon H_\varepsilon\big(K(\bar{\theta},\bar{\varphi}),\bar{\varphi}\big)$ have the same average and that the average of derivatives with respect to φ is zero. □

References

[AG90] E.L. Allgower and K. Georg. *Numerical continuation methods*, volume 13 of *Springer Series in Computational Mathematics*. Springer-Verlag, Berlin, 1990. An introduction.

[And98] M.A. Andreu. *The quasi-bicircular problem.* PhD thesis, Universitat de Barcelona, 1998.

[And03] M.A. Andreu. Preliminary study on the translunar halo orbits of the real earth–moon system. *Celestial Mechanics and Dynamical Astronomy*, 86(2):107–130, 2003.

[Arn63] V.I. Arnold. Proof of a theorem of A. N. Kolmogorov on the preservation of conditionally periodic motions under a small perturbation of the Hamiltonian. *Uspehi Mat. Nauk*, 18(5 (113)):13–40, 1963.

[AS99] M.A. Andreu and C. Simó. Translunar halo orbits in the quasibicircular problem. In *The Dynamics of Small Bodies in the Solar System*, pages 309–314. Springer, 1999.

[CCdlL13] R. Calleja, A. Celletti, and R. de la Llave. A KAM theory for conformally symplectic systems: efficient algorithms and their validation. *J. Differential Equations*, 255(5):978–1049, 2013.

[CCGdlL22] R. Calleja, A. Celletti, J. Gimeno, and R. de la Llave. Efficient and accurate KAM tori construction for the dissipative spin-orbit problem using a map reduction. *J. Nonlinear Sci.*, 32(1):1–40, 2022.

[CCH21] R. Calleja, M. Canadell, and À. Haro. Non-twist invariant circles in conformally symplectic systems. *Communications in Nonlinear Science and Numerical Simulation*, 96:105695, 2021.

[CFdlL03a] X. Cabré, E. Fontich, and R. de la Llave. The parameterization method for invariant manifolds. I. Manifolds associated to non-resonant subspaces. *Indiana Univ. Math. J.*, 52(2):283–328, 2003.

[CFdlL03b] X. Cabré, E. Fontich, and R. de la Llave. The parameterization method for invariant manifolds. II. Regularity with respect to parameters. *Indiana Univ. Math. J.*, 52(2):329–360, 2003.

[CFdlL05] X. Cabré, E. Fontich, and R. de la Llave. The parameterization method for invariant manifolds. III. Overview and applications. *J. Differential Equations*, 218(2):444–515, 2005.

[CH14] M. Canadell and À. Haro. Parameterization method for computing quasi-periodic reducible normally hyperbolic invariant tori. In *F. Casas, V. Martínez (eds.),* Advances in Differential Equations and Applications, volume 4 of *SEMA SIMAI Springer Series*, pages 85–94. Springer, 2014.

[CH17a] M. Canadell and À. Haro. Computation of Quasi-Periodic Normally Hyperbolic Invariant Tori: Algorithms, Numerical Explorations and Mechanisms of Breakdown. *J. Nonlinear Sci.*, 27(6):1829–1868, 2017.

[CH17b] M. Canadell and À. Haro. Computation of Quasiperiodic Normally Hyperbolic Invariant Tori: Rigorous Results. *J. Nonlinear Sci.*, 27(6):1869–1904, 2017.

[Chi79] B.V. Chirikov. A universal instability of many-dimensional oscillator systems. *Phys. Rep.*, 52(5):264–379, 1979.

[CJ00] E. Castellà and À. Jorba. On the vertical families of two-dimensional tori near the triangular points of the bicircular problem. *Celestial Mech. Dynam. Astronom.*, 76(1):35–54, 2000.

[DDP03] D.J. Dichmann, E.J. Doedel, and R.C. Paffenroth. The computation of periodic solutions of the 3-body problem using the numerical continuation software AUTO. In G. Gómez, M. W. Lo, and J. J. Masdemont, editors, *Libration Point Orbits and Applications*, pages 489–528. World Scientific, 2003.

[dlL01] R. de la Llave. A tutorial on KAM theory. In *Smooth ergodic theory and its applications (Seattle, WA, 1999)*, volume 69 of *Proc. Sympos. Pure Math.*, pages 175–292. Amer. Math. Soc., Providence, RI, 2001.

[dlLGJV05] R. de la Llave, A. González, À. Jorba, and J. Villanueva. KAM theory without action-angle variables. *Nonlinearity*, 18(2):855–895, 2005.

[dlLO06] R. de la Llave and A. Olvera. The obstruction criterion for non-existence of invarian circles and renormalization. *Nonlinearity*, 19(8):1907–1937, 2006.

[DTT17] D.A. Dei Tos and F. Topputo. On the advantages of exploiting the hierarchical structure of astrodynamical models. *Acta Astronautica*, 136:236–247, 2017.

[FdlLS09] E. Fontich, R. de la Llave, and Y. Sire. Construction of invariant whiskered tori by a parameterization method. I. Maps and flows in finite dimensions. *J. Differential Equations*, 246(8):3136–3213, 2009.

[GHdlL14] A. González, À. Haro, and R. de la Llave. Singularity theory for non-twist KAM tori. *Mem. Amer. Math. Soc.*, 227(1067), 2014.

[GHdlL22] A. González, À. Haro, and R. de la Llave. Efficient and reliable algorithms for the computation of non-twist invariant circles. *Foundations of Computational Mathematics*, 22(3):791–847, 2022.

[GJSM01] G. Gómez, À. Jorba, C. Simó, and J. Masdemont. *Dynamics and mission design near libration points. Vol. III*, volume 4 of *World Scientific Monograph Series in Mathematics*. World Scientific Publishing Co. Inc., River Edge, NJ, 2001. Advanced methods for collinear points.

[GM01] G. Gómez and J.M. Mondelo. The dynamics around the collinear equilibrium points of the RTBP. *Phys. D*, 157(4):283–321, 2001.

[GMM02] G. Gómez, J.J. Masdemont, and J.M. Mondelo. Solar system models with a selected set of frequencies. *Astronomy & Astrophysics*, 390(2):733–749, 2002.

[HCF+16] À. Haro, M. Canadell, J.L. Figueras, A. Luque, and J. M Mondelo. *The parameterization method for invariant manifolds: From Rigorous*

Results to Effective Computations, volume 195. Applied mathematical sciences, 2016.

[HdlL06a] À. Haro and R. de la Llave. A parameterization method for the computation of invariant tori and their whiskers in quasi-periodic maps: numerical algorithms. *Discrete Contin. Dyn. Syst. Ser. B*, 6(6):1261–1300, 2006.

[HdlL06b] À. Haro and R. de la Llave. A parameterization method for the computation of invariant tori and their whiskers in quasi-periodic maps: rigorous results. *J. Differential Equations*, 228(2):530–579, 2006.

[HdlL07] À. Haro and R. de la Llave. A parameterization method for the computation of invariant tori and their whiskers in quasi-periodic maps: explorations and mechanisms for the breakdown of hyperbolicity. *SIAM J. Appl. Dyn. Syst.*, 6(1):142–207 (electronic), 2007.

[HdlLS12] G. Huguet, R. de la Llave, and Y. Sire. Computation of whiskered invariant tori and their associated manifolds: new fast algorithms. *Discrete Contin. Dyn. Syst.*, 32(4):1309–1353, 2012.

[Hen79] P. Henrici. Fast fourier methods in computational complex analysis. *SIAM Review*, 21(4):481–527, 1979.

[HM21] À. Haro and J.M. Mondelo. Flow map parameterization methods for invariant tori in hamiltonian systems. *Communications in Nonlinear Science and Numerical Simulation*, 101:105859, 2021.

[JM99] À. Jorba and J. Masdemont. Dynamics in the center manifold of the collinear points of the restricted three body problem. *Phys. D*, 132(1-2):189–213, 1999.

[KAdlL22] B. Kumar, R. L. Anderson, and R. de la Llave. Rapid and accurate methods for computing whiskered tori and their manifolds in periodically perturbed planar circular restricted 3-body problems. *Celestial Mech. Dynam. Astronom.*, 134(1):1–38, 2022.

[Kol54] A.N. Kolmogorov. On conservation of conditionally periodic motions for a small change in Hamilton's function. *Dokl. Akad. Nauk SSSR (N.S.)*, 98:527–530, 1954. Translated in p. 51–56 of *Stochastic Behavior in Classical and Quantum Hamiltonian Systems, Como 1977* (eds. G. Casati and J. Ford) Lect. Notes Phys. 93, Springer, Berlin, 1979.

[LV11] A. Luque and J. Villanueva. A KAM theorem without action-angle variables for elliptic lower dimensional tori. *Nonlinearity*, 24(4):1033–1080, 2011.

[MHO09] K. R. Meyer, G. R. Hall, and D. Offin. *Introduction to Hamiltonian Dynamical Systems and the N–Body Problem*. Springer–Verlag, 2nd edition, 2009.

[Mos62] J. Moser. On invariant curves of area-preserving mappings of an annulus. *Nachr. Akad. Wiss. Göttingen Math.-Phys. Kl. II*, 1962:1–20, 1962.

[OS87] A. Olvera and C. Simó. An obstruction method for the destruction of invariant curves. *Phys. D*, 26(1-3):181–192, 1987.

[Rüs76] H. Rüssmann. On optimal estimates for the solutions of linear difference equations on the circle. In *Proceedings of the Fifth Conference on Mathematical Methods in Celestial Mechanics (Oberwolfach, 1975), Part I. Celestial Mech.*, volume 14, pages 33–37, 1976.

[SM95] C. L. Siegel and J. K. Moser. *Lectures on celestial mechanics*. Classics in Mathematics. Springer-Verlag, Berlin, 1995. Translated from German by C. I. Kalme, Reprint of the 1971 translation.

[Sze67] V. Szebehely. *Theory of orbits. The Restricted Problem of Three Bodies.* Academic Press, 1967.

Departament de Matemàtiques i Informàtica, Universitat de Barcelona, Gran Via 585, 08007 Barcelona, Spain.
Email address: alvaro.fernandez@ub.edu

Departament de Matemàtiques i Informàtica and BGSMath, Universitat de Barcelona, Gran Via 585, 08007 Barcelona, Spain., Centre de Recerca Matemàtica, Edifici C, Campus Bellaterra, 08193 Bellaterra (Barcelona), Spain.
Email address: alex@maia.ub.es

IEEC & Departament de Matemàtiques, Universitat Autònoma de Barcelona, Av. de l'Eix Central, Edifici C, 08193 Bellaterra (Barcelona), Spain.
Email address: josemaria.mondelo@uab.cat